

ANALYSIS OF THE MAXIMUM FINITE TIME LYAPUNOV EXPONENT IN TIME DOMAIN USING DATA FROM TORSO STABILITY TESTS

A thesis presented to the faculty of the Graduate School of
Western Carolina University in partial fulfillment of the
requirements for the degree of Master of Science in Technology

By
Chaoke Dong

Advisor: Dr. Martin L. Tanaka
Department of Engineering & Technology

Committee Members:
Dr. Michael S. June, Department of Engineering & Technology
Dr. Yanjun Yan, Department of Engineering & Technology

November 2015

To my families, for their endless support

ACKNOWLEDGEMENTS

I would like to give special thanks to my thesis director, Dr. Martin L. Tanaka, whose guidance and support made all my research possible. I am really grateful that he introduced the fantastic topic – torso stability to me, so that I can have this valuable opportunity to work on it. I have really good experience to work with Dr. Tanaka. His passion for research has always been an encouragement for me, and he is always willing to help me. I learned a lot from our discussions.

My thanks also go to my committee members, Dr. Michael S. June and Dr. Yanjun Yan. Although they are very busy, they never rejected me whenever I needed to talk to them about my research. Especially Dr. Yanjun Yan, she gave me some suggestions on how to organize Matlab codes and reduce the runtime of codes.

I would like to extend my thanks to all the other professors who taught me during my graduate years, Dr. Sudhir Kaul, Dr. Aaron Ball, Dr. Guanghsu Chang, Prof. Michael Clare, and Dr. Robert Adams. I really enjoyed their class and learned a lot from their classes. I would also like to thank all my classmates in the MST program for the beneficial discussions we had together.

In addition, I would like to express my sincere gratitude to the Western Carolina University Graduate School for awarding research Grants to Dr. Tanaka. Funds from these grants were used to purchase the materials used to improve the Basin of Stability chair in the research. I would also like to thank Mr. Monty Graham for providing assistance and help purchasing the materials needed to complete this research.

Finally, I would like to thank my husband, and my other family members for their endless support.

TABLE OF CONTENTS

List of Tables	vi
List of Figures	vii
Abstract	ix
CHAPTER 1: Introduction	1
CHAPTER 2: Literature Review	4
2.1 Low Back Pain (LBP).....	4
2.2 Core Stability	4
2.3 Current Method.....	6
2.3.1 Torso Stability Experiments and Experimental Devices.....	6
2.3.2 Mathematical Model and Simulation of Torso Stability.....	10
2.3.3 Techniques Used to Study The Dynamical System	13
2.4 Basin of Stability (BoS)	16
CHAPTER 3: Methods	17
3.1 Research Plan.....	17
3.2 Establishing The Testing Environment.....	17
3.3 Conducting The Test.....	28
3.3.1 Objective of Torso Stability Experiment	28
3.3.2 Test Subjects	28
3.3.3 Preliminary Test.....	29
3.3.4 Full Scale Test.....	34
3.4 Data Collection	36
3.5 Data Analysis.....	37
CHAPTER 4: Results and Discussion	39
4.1 Analysis and Results of Preliminary Data	39
4.2 Analysis and Results of Full Scale Study	44
4.2.1 Different Stages of Stability Test.....	45
4.2.2 Effect of Gender on The Lyapunov Exponent	52
4.2.3 Effect of Different Filters on The Lyapunov Exponent	55
4.2.4 Effect of Different Evolution Times on The Lyapunov Exponent.....	57
CHAPTER 5: Conclusion and Future Work.....	60
Bibliography	62
Appendices.....	67
Appendix A: Main Code for How to Calculate The Lyapunov Exponent in Time Domain	67

Appendix B: Main Code for How to Align The Time Plots with The Lypunov Exponent Plots at Assigned Time Zero..... 70

Appendix C: Main Code for How to Average the Lypunov Exponent..... 73

LIST OF TABLES

3.1	The basic information of test subjects	29
4.1	Lists of cutoff frequencies for different filters.....	56

LIST OF FIGURES

1.1	Basins of stability found from mathematical models of seated torso stability. (a) The finite time Lyapunov exponent field shows Lagrangian coherent structures (LCS); (b) The LCS viewed from the top	3
2.1	The anatomy of core	5
2.2	A subject positioned on an unstable seat in a test apparatus.....	7
2.3	Wobble chair (above) and spring layout (below)	8
2.4	The integrated configuration of the BoS chair.....	9
2.5	Main parts of the BoS chair	10
2.6	(a) Wobble chair with the movement of lumbar spine and (b) Simplified mathematical model.....	11
2.7	(a) Time plot for simulated experimental trials. (b) The trajectories in state space	12
2.8	How two initially close trajectories diverge or separate	13
3.1	Image of the wood frames arranged around the chair.....	18
3.2	Locking up three safety frames.....	18
3.3	Using clamp to open and close the safety frame easily	19
3.4	(a) Adjust tool; (b) Step stool.....	20
3.5	Example of Xsens software showing data readouts (left) and a 3D representation of the sensor heading (right).	21
3.6	Gyroscopic sensor is fixed behind the seat	21
3.7	(a) The beam frame (b) The support rope hanging on the beam and (c) Support feet.....	23
3.8	(a) Using eyelets to hold the foam; (b) Using small wood piece to hold the foam	24
3.9	Grip tape.....	25
3.10	(a) Foam tape for sharp edge; (b) Foam tape for sharp tip	25
3.11	Front panel of custom LabView program.....	26
3.12	Block diagram of custom LabView program.....	27
3.13	(a) The subject held the rope to keep balance. (b) The subject kept balance with arm crossed. (c)The subject fell	30
3.14	Basin of stability test protocol	32
3.15	Basin of stability test protocol (continue).....	33
3.16	Testing sheet	35
3.17	Raw data collected from LabView	36
3.18	Flow chart depicting how the FTLE is calculated and plotted	38
4.1	Time plots for 5 trials.....	40
4.2	Plots in state space	40
4.3	Plot of angle vs. time and Lyapunov exponent at different evolution time	41
4.4	Time plots and FTLE plots in the same period.....	42
4.5	Average FTLE vs. time with evolution time 50 milliseconds	44
4.6	Time plot for 55 trials and lining up at $t = 0$	45
4.7	Centered time plot for 55 trials and lining up at $t = 0$	46
4.8	State space plot	47
4.9	Different stages of stability test	49
4.10	FTLE field with reverse time flow.....	50

4.11	State-space-average Lyapunov exponent from mathematical model	51
4.12	Average FTLE at evolution time 50 milliseconds for male subject	53
4.13	Average FTLE at evolution time 50 milliseconds for female subject	53
4.14	Average FTLE vs time at evolution time = 50 ms for different gender subject	54
4.15	Average Lyapunov exponent plots with different filters (male, evolution time = 50 ms)...	57
4.16	Average FTLE plots with different evolution times	58
4.17	Normalized average FTLE vs time with different evolution time	59

ABSTRACT

ANALYSIS OF THE MAXIMUM FINITE TIME LYAPUNOV EXPONENT IN TIME DOMAIN USING DATA FROM TORSO STABILITY TEST

Chaoke Dong, M.S.T.

Western Carolina University (November 2015)

Director: Dr. Martin L. Tanaka

Low back pain (LBP) is a common health problem that affects most people during their life. The goal of this research is to track the dynamics of seated stability through the falling region and determine how the maximum finite time Lyapunov exponent (FTLE) changes over time. The FTLE describes how quickly two initially close points in state space diverge. Human torso stability tests were conducted using an unstable sitting apparatus capable of attaining large deflection angles. Angle data was collected using a gyroscopic sensor and Matlab was used to calculate the FTLE in the time domain. The analysis results for the Lyapunov exponent in the time domain were consistent with the results found in state space. Deterministic behavior of the dynamical system was also detected. A suite of parameters were investigated in the data analysis. The Lyapunov exponent was found to be sensitive to changes in evolution time but not sensitive to the cutoff frequency of the low pass filter when it was above 3.2 Hz. A key point of this research was to understand how the Lyapunov exponent changed with time as it approached a critical event. Tracking the Lyapunov exponent in the time domain may be a useful indicator to predict a future event. Moreover, this approach may be generalizable to other dynamic systems that have critical transitions. This research helps to better understand torso stability and build onto the foundation of knowledge to diagnose and prevent LBP.

CHAPTER 1: INTRODUCTION

Low back pain (LBP) is a very common problem in modern health care. About 40% of people worldwide have reported LBP at some point of their lives [1]. This number is ever greater in developed countries with four out of five people experiencing LBP [2]. LBP affects people of all ages, from adolescent to the elderly. The prevalence of LBP on adolescents is lower than adults, but has been increasing in recent years [3]. It is difficult to estimate the incidence of LBP because LBP may recur over time after the LBP patient has alleviated pain using medication, physical therapy, or surgery. LBP is one of top 10 reasons that people consult a physician [4]. Furthermore, LBP is also a major cause of activity limitations and work absence, which leads to a high economic burden on individuals, families, and government [3, 5]. In the United States, it has been estimated that about 100 to 200 billion dollars is lost each year because of LBP [6, 7, 8].

Often the cause of LBP is obscure and difficult to distinguish, since many different factors may lead to the same or similar symptoms. Torso instability has been associated with LBP and is the topic of interest for researchers. Although there seems to be a link between LBP and torso instability, the relationship has not been clearly understood [9]. Therefore, a series of studies have been performed to better understand this relationship [10, 11, 28, 30]. Using various unstable sitting apparatus, the torso stability was quantified. Test subjects maintained balance on the chair while their movement was recorded. Movement was analyzed using kinematic variability parameters and the maximum finite time Lyapunov exponent.

From the studies above, it seems that the maximum finite time Lyapunov exponent is a common and useful tool to quantify torso stability from time series data. The Lyapunov exponent measures the divergence rate between two points which are initially close in the state space. Generally, previous researchers have calculated the maximum Lyapunov exponent as a single scalar value [10, 11, 31, 39, 40] with the primary goal of identifying the presence of deterministic chaos. This was accomplished by calculating the average divergence rate over the entire time series. However, this approach does not show how the dynamic system changes with time. It assumes a constant divergence rate through the entire time series that may be simply represented by the average value.

In addition, mathematical models have been developed [12]. Simulations were carried out to generate time series data, from which the maximum finite time Lyapunov exponents were calculated. The magnitude of the finite time Lyapunov exponent was found to change with respect to its location in state space [13 - 16]. When plotted, the finite time Lyapunov exponent (FTLE) field shows structural features that aligned with the dynamical behavior of the system (Figure 1.1). Although the state space representation of a system shows more information about the system dynamics than a single scalar value, it still does not take into account the component of time.

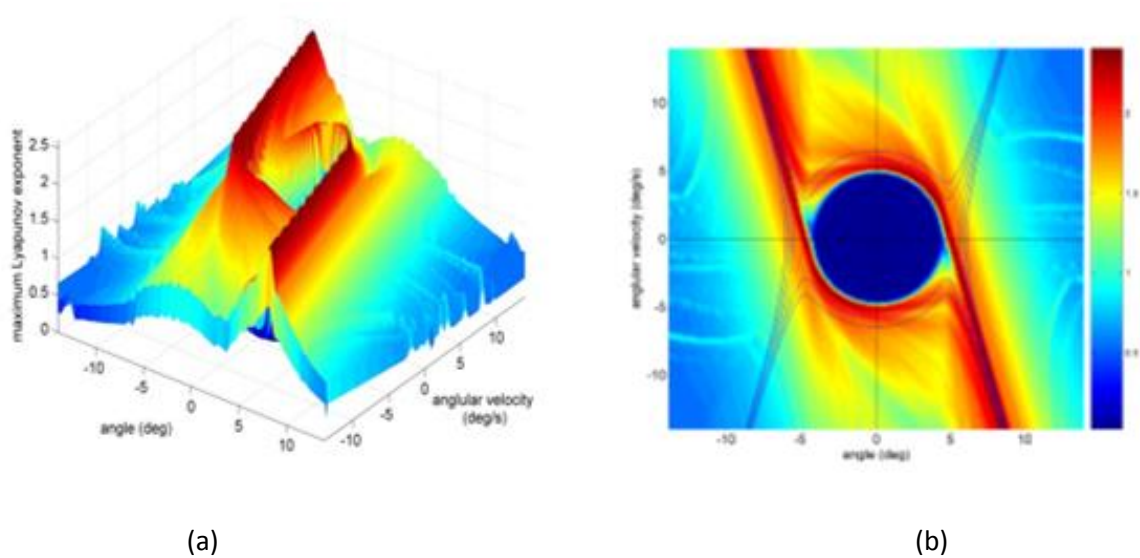


Figure 1.1: Basins of stability found from mathematical models of seated torso stability. (a) The finite time Lyapunov exponent field shows Lagrangian coherent structures (LCS) [13]; (b) The LCS viewed from the top [13, 45]

The purpose of this research is to track the dynamics of seated stability through the falling region and to determine how the maximum finite time Lyapunov exponent changes over time. Specifically we are interested in understanding how the FTLE changes prior to an unstable event. In our case, this event is the loss of stability that results in falling during a torso stability test. If we are able to identify features of the FTLE that occur prior to a loss of stability, this may be useful in predicting and possibly preventing spinal instability injuries and the resulting LBP.

CHAPTER 2: LITERATURE REVIEW

2.1 Low Back Pain (LBP)

The low back includes the lumbar region of spine, surrounding muscles and connective tissue. Its main functions are to provide structural support, enable torso movement, and protect the spinal cord [18]. LBP refers to the disorder of muscles, tissue and bones in low back which results in pain [19]. Symptoms usually are back stiffness, numbness of the lower extremities and difficulty moving or standing straight. It is commonly diagnosed by X-ray test, CT scanning or MRI scanning. One common cause of LBP is back muscle strain or ligament strain which is developed by some movements, like lifting a heavy object, twisting, or forward-bending [20]. As early as 1995, Adam and Dolan proposed that mechanical fatigue damage may be the underlying reason for LBP [21]. The current treatment for LBP is medication, physical therapy, and surgery, which may alleviate the pain of patient, but these treatments do not always eradicate the LBP based on the patients' experiences. Often the cause of LBP is unknown and cannot be diagnosed and referred to as idiopathic LBP [22].

2.2 Core Stability

The core of body consists of abdominal structures, spine, pelvis, and hip (Figure 2.1). Core stability is described by Kibler et al. as “the ability to control the position and motion of the trunk over the pelvis and hip to allow optimum production, transfer and control of force and motion to the terminal segment” [23]. The lumbar spine is mainly used to keep an upright

posture and stability of the torso. This is important in dynamic sports such as running, tennis, and soccer, as well as activities of daily living. [23, 24].

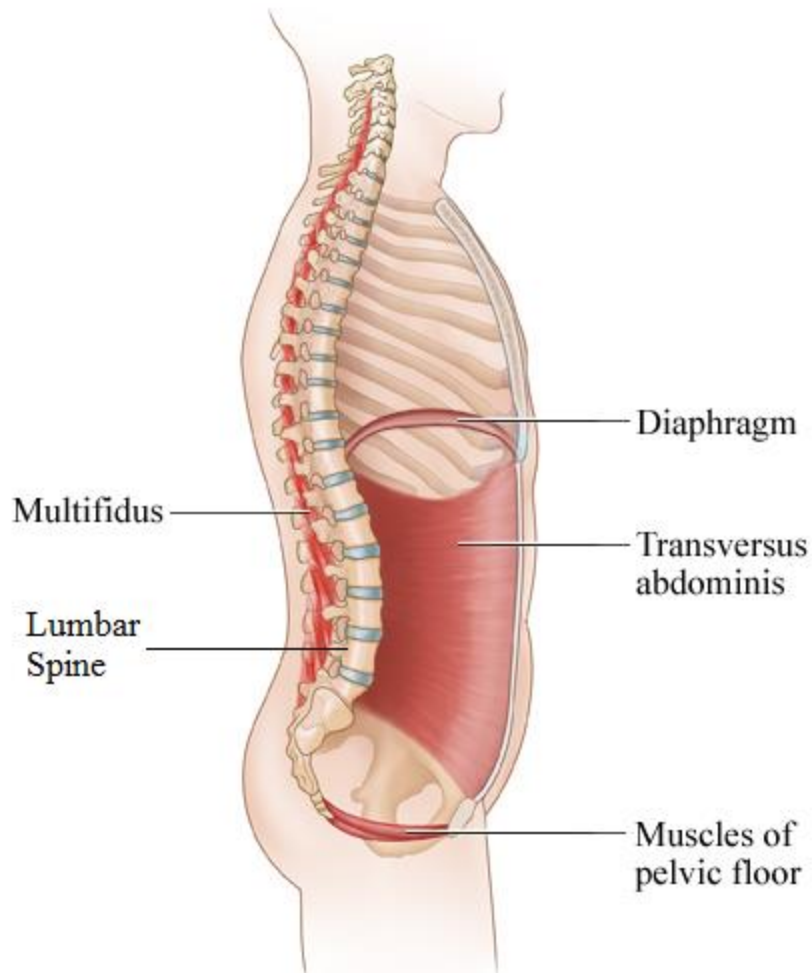


Figure 2.1: The anatomy of core [25]

The muscles and joints of the pelvis and spine play a key role in stabilizing and balancing human movement. Core instability can result in injury to the low back. However, the risk of low back injury can be significantly reduced by strengthening the muscle of the core [26]. As a result, increasing core stability is an important method used in rehabilitation of LBP [26].

Core stability is so important that numerical investigations into the relationship between core stability and athletics have been conducted. Joshua studied the effect of core stability exercises as a possible treatment for athletes with LBP. Although he did not establish the relationship between exercise and LBP, the core exercises were shown to improve the core muscle strength and endurance [27]. People have also performed other experiments to measure core stability, and one of them is a torso stability experiment.

2.3 Current Method

2.3.1 Torso Stability Experiments and Experimental Devices

Torso stability is the ability to keep stable movement and upright posture, and it is controlled by muscle recruitment, active muscle stiffness, and reflex response in low back area [28]. In order to stabilize the spine, the spinal column, spinal muscles, neural control unit, and core muscles need to coordinate their efforts together. Spinal instability is defined as loss of the ability to maintain its normal pattern of displacement of the spinal under load without pain and deformity by Panjabi [29]. Granata et al. found that the fatigue induced by lifting has a negative influence on spinal stability [28].

In 2000, Cholewicki et al. developed an experimental method to quantify the postural control capability of the lumbar spine using an unstable sitting apparatus (Figure 2.2). This unstable apparatus was equipped with a seat, polyester resin hemispheres and a support for the legs and feet. By decreasing the diameter of the hemisphere, the difficulty level of the task was increased. They recorded the center of pressure (COP) and quantified the torso stability using

statistical analysis of the kinematic variability [30]. From this method, the mechanism underlying control of the lumbar region can be better understood by studying the balance in a seated posture.

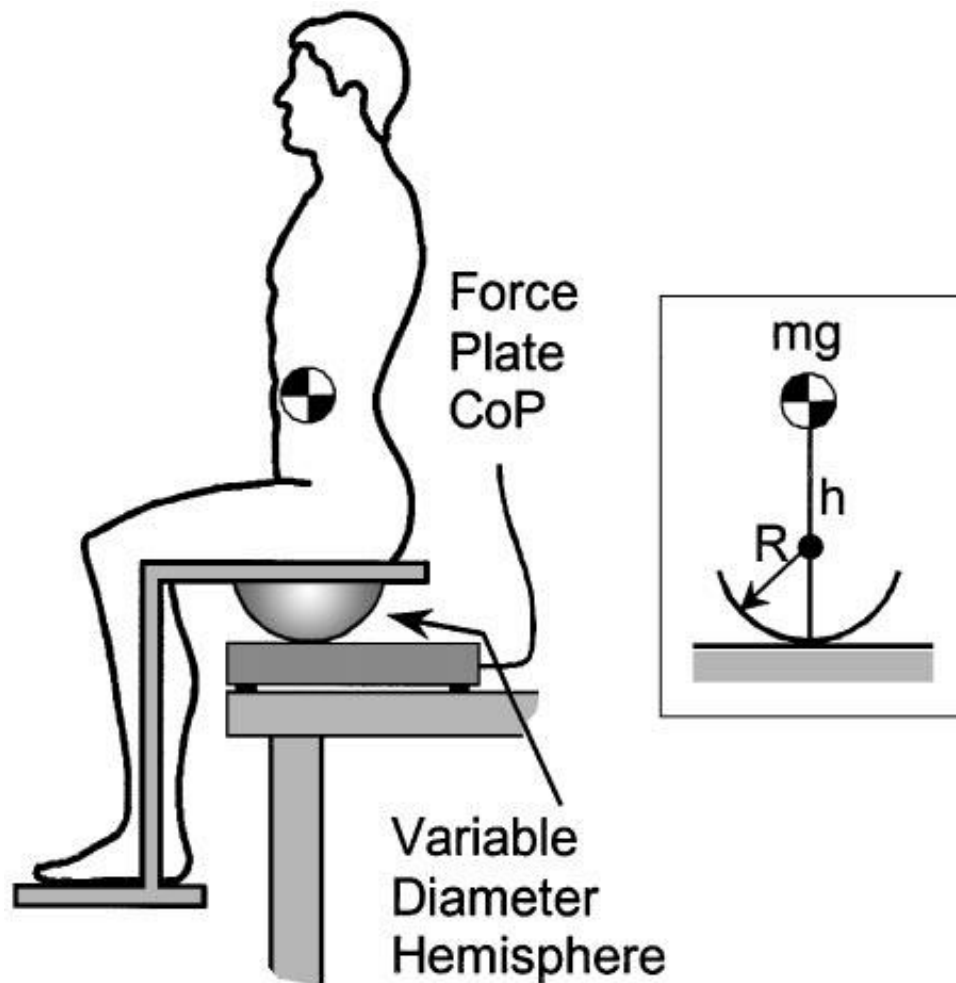


Figure 2.2: A subject positioned on an unstable seat in a test apparatus [30]

The Threshold of Stability (ToS) was investigated and evaluated as an indicator for human torso stability using another unstable apparatus – the wobble chair (Figure 4). Results indicated that ToS is sensitive to the difference of visual feedback by assessing the maximum Lyapunov exponents, which might be a diagnostic method for LBP [10].

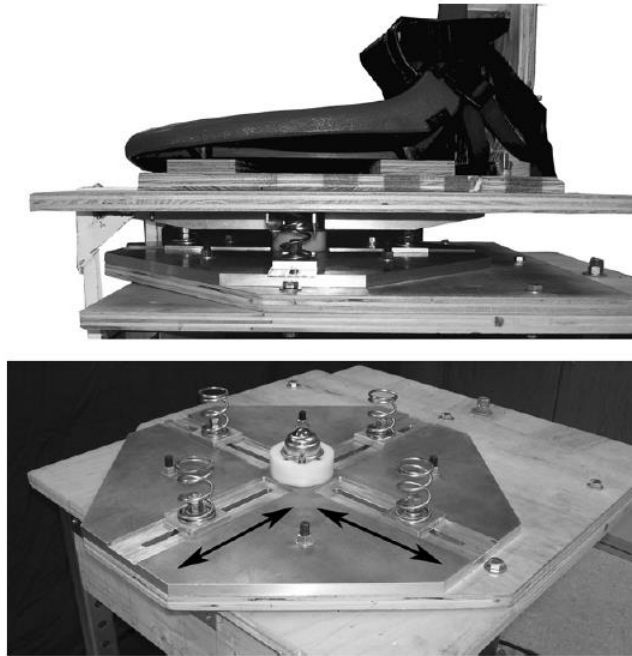


Figure 2.3: Wobble chair (above) and spring layout (below) [32]

Also using wobble chair, the torso stability was quantified by challenging the stability control of the test subject. This mechanical assessment method is a valuable tool for identifying individuals at risk for LBP [11]. The wobble chair includes a seat and seat supporting structures, including springs, central ball joint, etc. The principle of the wobble chair is to change the task difficulty level by changing the distance of spring from center. Experiment data were collected to analyze the kinematic variability and non-linear stability control [32].

A new device, named Basin of Stability Chair (Figure 2.4 and Figure 2.5), was designed and built by a previous WCU graduate student [17]. The BoS chair is a torso stability test apparatus based on the wobble chair (Figure 2.3) which was used for stability test in previous researches [11, 14]. The mechanism of BoS chair is very similar to the wobble chair. It includes

a seat, seat slider, pivot ball joint, enclosed springs, spring traverses, safety frames, and adjust tool. The seat allows test subject to sit on one side and kneel down on the other side, which assures that the test subject have to use their torso to keep balance. The seat can slide backward and forward along the seat slider. This can make sure that the subject's mass center is over the pivot ball. The pivot ball joint allows the seat to rotate freely in 2-dimension, roll and pitch, and slightly in the third dimension, yaw. The springs under the seat are at the left, right, front, and back side of the center. The distance from the spring to the central ball joint can be changed using an adjust tool. This can be used to compensate for anatomical differences in subjects [11] and allow experiments to be conducted at a specified difficulty level. To avoid large deformation and possible low back injury due to falling, a safety frame was built to surround the BoS chair. After the BoS chair was finished it was used to conduct a threshold of stability study [17].

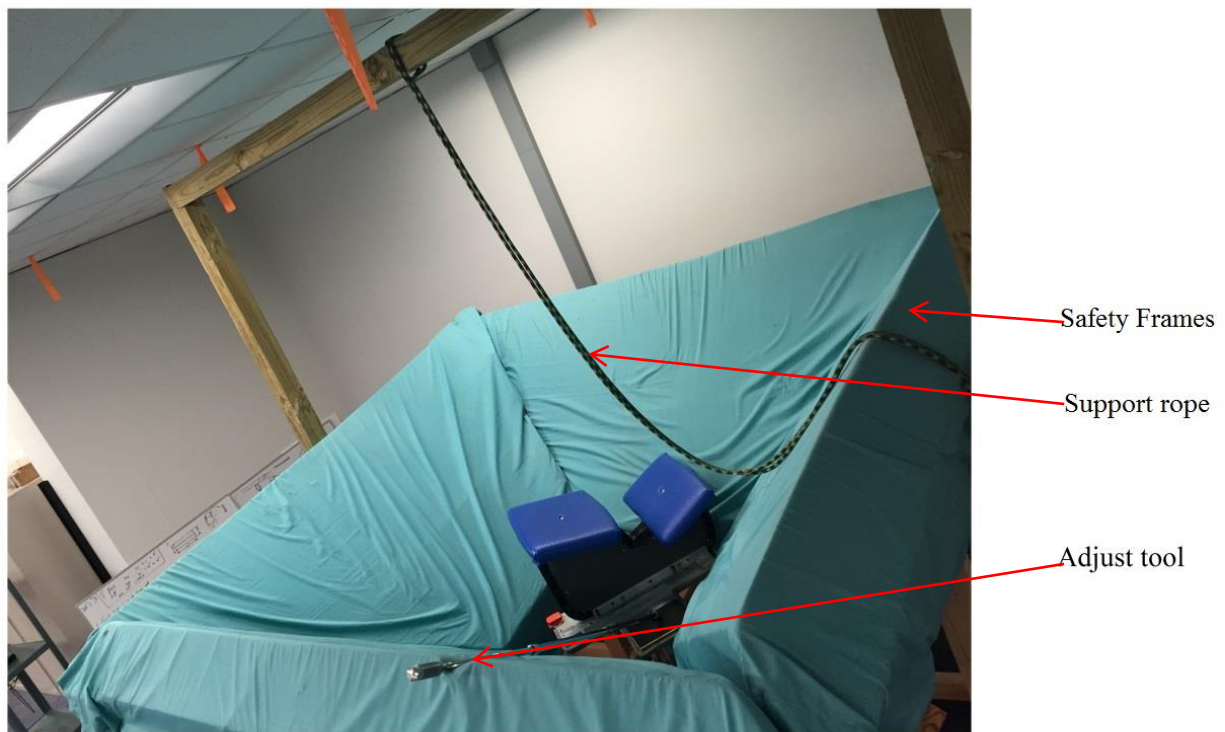


Figure 2.4: The integrated configuration of the BoS chair

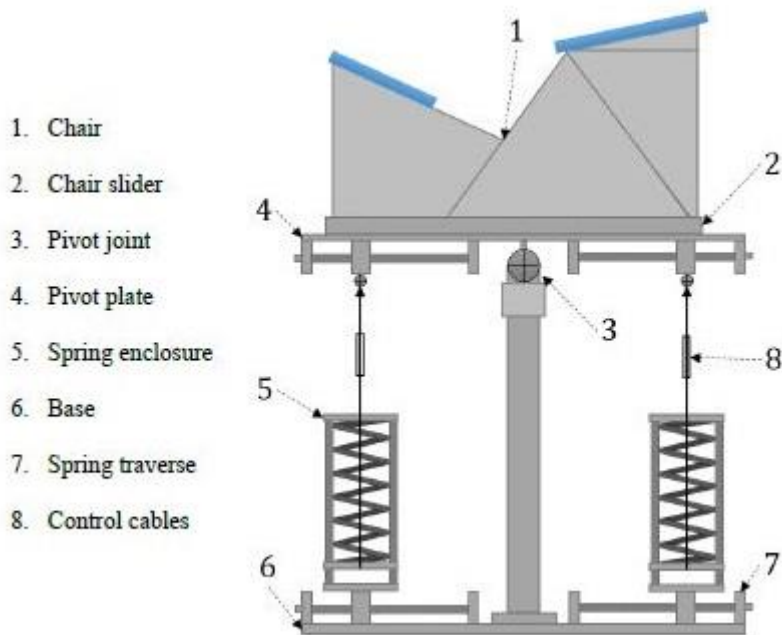


Figure 2.5: Main parts of the BoS chair [17]

There are three major differences between the BoS chair and the wobble chair. First, the BoS chair allows for large angular deflections. This allows movement of the subject to be tracked during falling. This is also the reason why the seating was changed from sitting to kneeling. Second, the seat of BoS chair can rotate about the vertical axis to a limited degree; however the wobble chair has very little ability to rotate in transverse plane. Third, the spring for the BoS chair is longer and stronger than the wobble chair, which allows us to set more difficulty levels for the test.

2.3.2 Mathematical Model and Simulation of Torso Stability

Tanaka, Ross and Nussbaum created a mathematical model of a test subject sitting on the wobble chair (Figure 2.6 (a)). Figure 2.6(b) shows the simplified mathematical model. The second order

differential equation was obtained using the physical force analysis. Physiologically, the limited gain controller C in the equation represents the limited muscle strength of the abdominal and spinal extensor muscles [13].

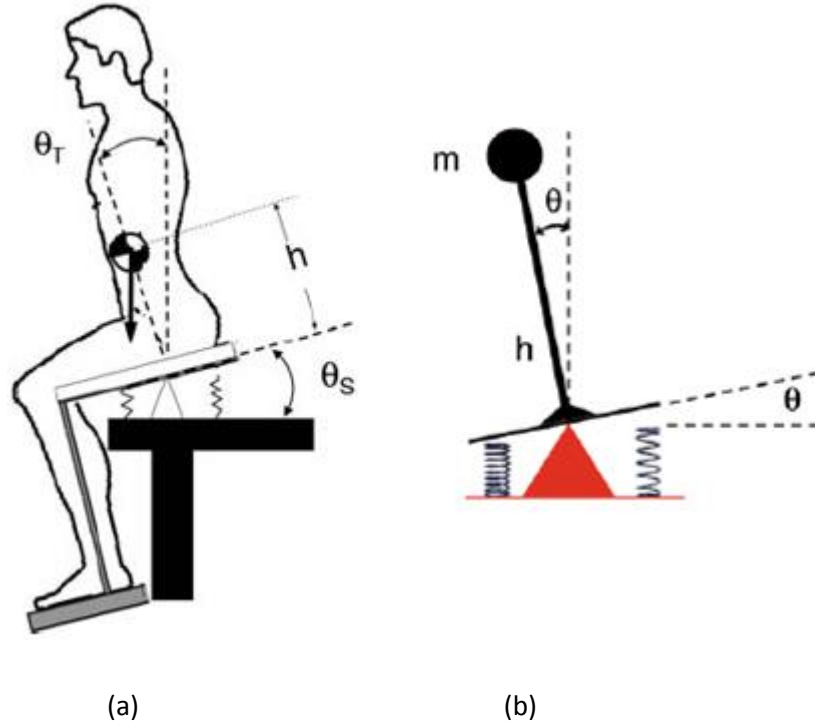


Figure 2.6: (a) Wobble chair with the movement of lumbar spine and (b) Simplified mathematical model [13]

$$\ddot{\theta} = \frac{1}{mh^2} (mgh \sin\theta - kd^2 \sin\theta - C(\theta, \dot{\theta}) + N) \quad (2.1)$$

Where $\ddot{\theta}$ is angular acceleration, m is a concentrated body mass, g is acceleration of gravity, h is height from seat to body center, θ is rotation angle, $\dot{\theta}$ is angular velocity, k is spring constant, d is distance of spring from central ball joint, N is system noise, and C is the equation for the limited gain proportional-derivative control and it is given by

$$C(\theta, \dot{\theta}) = G_d \dot{\theta} + \begin{cases} G_p \theta & \text{if } |\theta| < \theta_{cr} \\ \tau_{p_max} & \text{otherwise} \end{cases} \quad (2.2)$$

Where G_d is the derivative gain constant, θ_{cr} is equal to $\frac{\tau_{p_max}}{G_p}$, the smallest angle at which the maximum gain is achieved, G_p is proportional gain constant, τ_{p_max} is maximum torque producible by proportional gain.

Using the equations above, a dynamic simulation was created to generate time series data in Matlab. The angular position data was generated with respect to time, and the velocities were numerically calculated. Thus, all data for constructing the state space were available. The results are showed in Figure 2.7. Nonlinear stability analysis was conducted to calculate the maximum Lyapunov exponents. The separatrices and basins of stability were identified using the Lagrangian Coherent Structures method.

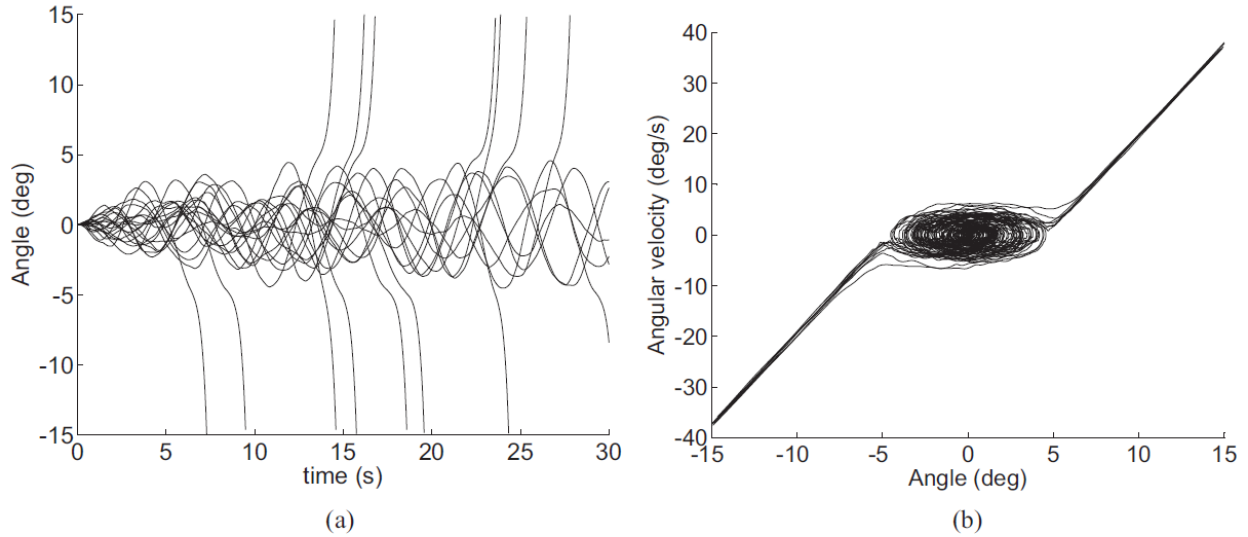


Figure 2.7: (a) Time plot for simulated experimental trials. (b) The trajectories in state space [13]

2.3.3 Techniques Used to Study The Dynamical System

The maximum finite time Lyapunov exponent is a parameter that can be used to calculate the local dynamic stability. Researchers have used this parameter as a method to detect the deterministic chaos in a dynamical system [10-13, 28, 30-32, 38-40]. The maximum finite time Lyapunov exponent is a quantity that represents the rate of exponential divergence or convergence of initially close points in the state-space of a dynamical system. Figure 2.8 shows the divergence rate of two trajectories, and it is given by:

$$|d(\Delta t)| = |d(0)|e^{\lambda\Delta t} \quad (2.3)$$

where λ is the Lyapunov exponent, $d(t_i)$ is the distance between the reference point and its nearest neighbor at $t = t_i$, d_0 is the distance between the reference point and its nearest neighbor at $t = 0$, and Δt is the evolution time, which equals to $t_i - t_0$.

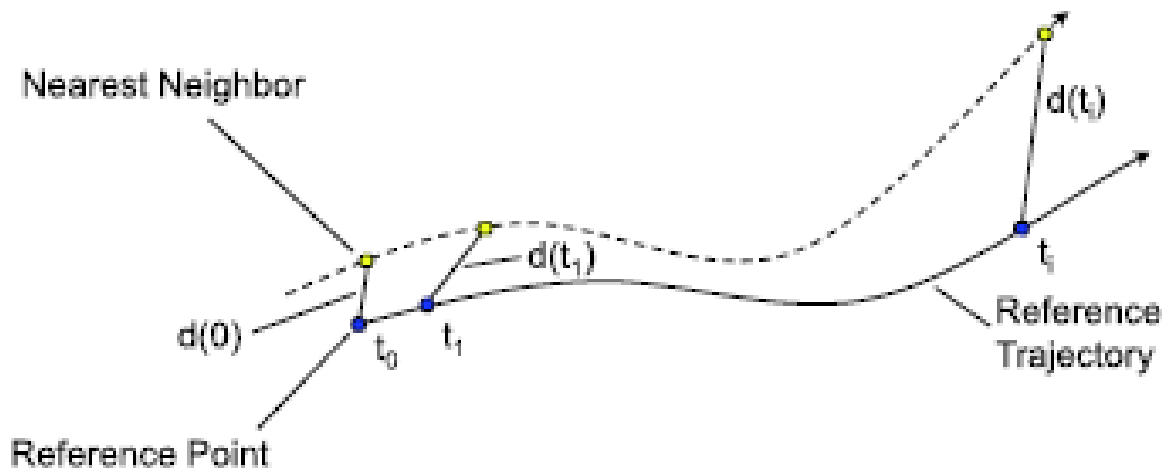


Figure 2.8: How two initially close trajectories diverge or separate [1]

The Lyapunov exponent is an indicator of system stability, and a larger value of the Lyapunov exponent indicates a less stable behavior in the dynamical system. For

multidimensional dynamical systems, the Lyapunov exponent may be different in the different dimensions with the same initial separation vector, and the largest one is called the maximum Lyapunov exponent, which is used as the important and useful indicator for distinguishing chaos. If a system is found to exhibit deterministic chaos, it makes prediction of the future behavior of a dynamical system possible.

If the equations of motion for a dynamical system are known, the maximum Lyapunov exponent can be numerically calculated using the definition equation (2.3) [34, 35]. However, this method cannot be directly applied to the experimental time series data, since the equations of motion cannot not be obtained easily in a real system. Therefore, a method to calculate the maximum Lyapunov exponent for experimental data needed to be investigated.

Wolf et al. [36] presented the first algorithm to determine the maximum Lyapunov exponent from experimental time series data sets in 1985. This algorithm involves examining orbital divergence on a small length scale and reconstructing the state space using an approximate Gram-Schmidt-reorthonormalization (GSR) procedure. The major disadvantage in their algorithm is that the estimation of the maximum Lyapunov exponent is sensitive to the number of the observations, the dimension of the measurement, and the evolution time.

In 1993, Rosenstein et al. [37] recognized the drawbacks in Wolf's algorithm and provided a new method of calculating the maximum Lyapunov exponent for the small data set. The method can be divided into four steps: reconstructing the attractor dynamics, locating the nearest neighbor of each point on the trajectory, tracking the exponential divergence of nearest

neighbors, and calculating the maximum Lyapunov exponents using least-square fit. This algorithm is fast, easy to implement and robust to change in embedding dimension, size of data set, reconstruction delay, and noise level.

In 2000, Dingwell et al. conducted experiments on human passive walking on a motorized treadmill and applied time-series analysis techniques to data collected from human locomotion. They used Rosentstein's algorithm to estimate the maximum FTLE in order to quantify the local dynamic stability of human walking kinematics [38]. In 2006, England and Granata did a similar stability test of human walking about gait speed, and they also used Rosentstein's algorithm to quantify the stability of system with the maximum FTLE and reached the conclusion that a smaller values of the maximum FTLE indicate more stable walking dynamics [39].

Tanaka et al. assessed torso stability by calculating the maximum Lyapunov exponent as a single scalar value from experiment data. They found that wobble chair stability negatively correlated to the maximum Lyapunov exponent [11]. Lee et al. performed a similar stability test and analyzed the nonlinear stability by computing the maximum Lyapunov exponent. It was found that the maximum Lyapunov exponent provided excellent measures for intra-session analysis [40]. In the same year, Lee et al. recorded the data from the subject sitting on the wobble chair with externally applied exertion forces from different directions. They evaluated the postural control of trunk by calculating the maximum Lyapunov exponent and found that the value of Lyapunov exponent was increased as the exertion forces increased. In addition, the

measures including the Lyapunov exponent indicated that the performance of postural control during flexion exertions was poorer than extension exertions [31].

2.4 Basin of Stability (BoS)

Before introducing the basin of stability, some related terms need to be explained. First the definition of a dynamical system will be introduced. In general, a dynamical system is a set of components whose state changes over time. There are two different kinds of dynamical systems: discrete and continuous. They can also be categorized into linear and nonlinear dynamical systems [41, 42, 43].

In a dynamical system, an attractor is a subset of the state space which trajectories are drawn towards as time increases, although the initial conditions of trajectories may be quite different [44]. Basin of attraction of an attractor is the region which all conditions approach after each different condition evolves. Basin of stability comes from the idea of basin of attraction. BoS, as the name implies, refers to a region in state space in which people are able to keep stability or balance. Beyond this region, people may lose stability and fall during a torso stability test.

Tanaka and Ross (2009) located the separatrices and basin of stability from time series data by calculating the maximum FTLE in the state space [13]. This may be used to develop a better tool to improve diagnosis and treatment of LBP.

CHAPTER 3: METHODS

3.1 Research Plan

This research consists of three major components. The first component was to establish the testing environment to make sure that the stability test could be performed successfully. The second component was designing the test protocol and then conducting the torso stability tests. The third component was the development of new methods to analyze the experimental data. Customized Matlab code was created to analyze the data.

3.2 Establishing The Testing Environment

The first step in establishing the test environment was to move the BoS chair to the test laboratory and reassemble the safety frames. Unfortunately, when the safety frames were originally taken apart to be moved into storage, no one labeled the four frames so the proper arrangement for reassembly could not be easily determined. Multiple configurations were tested, but each seemed to not fit well. Finally, the correct order was identified by inspecting a photograph in the thesis of the previous graduate student who built the original device. In the photograph the wood grain was visible and could be used to identify the proper arrangement of the wooden frames (Figure 3.1).



Figure 3.1: Image of the wood frames arranged around the chair [17]

In order to improve stability, the feet of three sides of the frame were attached together using small wood plates and screws (Figure 3.2). This made the safety frame more stable and firm enough to safely hold the subject when they fell.



Figure 3.2: Locking up three safety frames

In order to open and close the safety frame easily, a latch action clamp was added to the fourth side of safety frame which acted like a door. It securely connected the fourth component of the safety frame with the other three sides of the frame. To secure the clamp better, it was attached to a wood plate and the wood plate was screwed to the safety frames (Figure 3.3).



Figure 3.3: Using clamp to open and close the safety frame easily

The difficulty level of the task was changed by adjusting the distance between the spring and the center of the BoS chair using a specialized tool – adjust tool. The adjust tool (Figure 3.4 (a)) consists of one speed handle, two extension bars, one universal joint, and one 0.5 inch 12-point socket [17]. A step stool was purchased (Figure 3.4 (b)) to assisting the subject when

climbing on the BoS chair. In addition, the stool helped the tester to adjust the task difficulty levels because the safety frames were too high to reach over without a step stool.



(a)



(b)

Figure 3.4 (a) Adjust tool; (b) Step stool

Then the application software of the gyroscopic sensor (MTi – 28A53G25 motion tracker, Xsens North America Inc.) was installed in the computer and used for the test. The sensor was tested to make sure that it ran normally. When the sensor worked well, the testing results looked like the image in Figure 3.5.

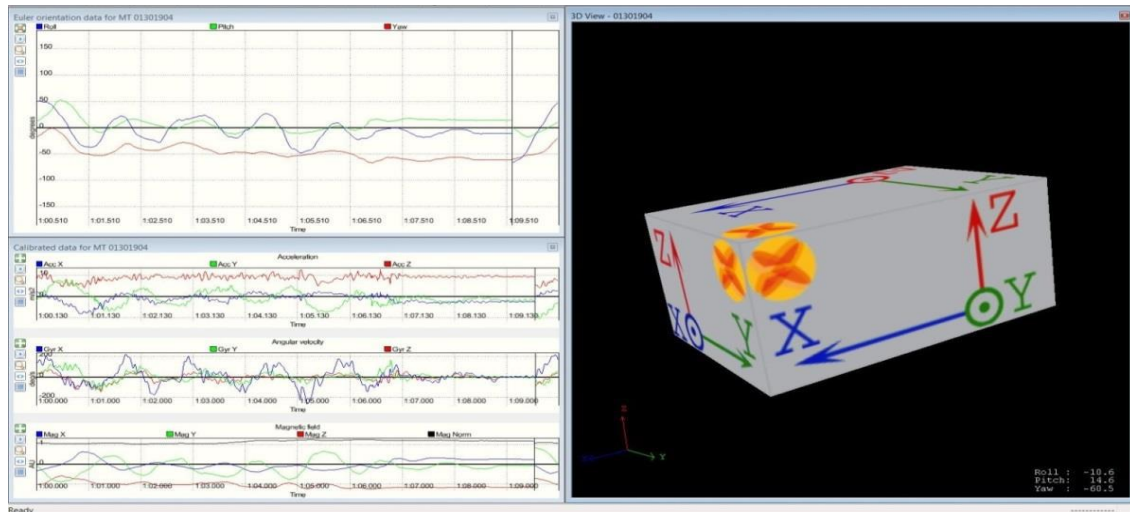


Figure 3.5: Example of Xsens software showing data readouts (left) and a 3D representation of the sensor heading (right).

After setting up the sensor, the next step was to fix the sensor to the BoS chair. A small hole in the pivot plate of the BoS chair was drilled and tapped. Then the sensor was attached to the pivot plate behind the seat using a screw (Figure 3.6).

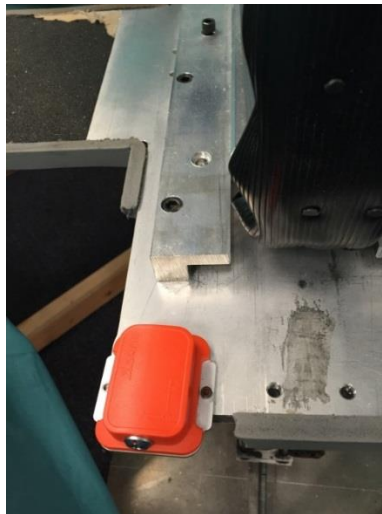


Figure 3.6: Gyrosopic sensor was attached behind the seat

To prepare for the test, a post and beam structure was built for hanging the support rope, which was used by the subjects during the test. First the height and width of the frame were measured. Then three pieces of 4" by 4" wood were purchased and sawed to the size needed. Afterwards, all pieces of the wood were assembled together and the BoS chair was placed between them. The support rope was hung from the beam, and support feet were installed at each side of the frame to prevent it from falling (Figure 3.7). The post and beam structure was also screwed to the frame.



(a)



(b)



(c)

Figure 3.7: (a) The beam frame (b) The support rope hanging on the beam and (c) Support feet

The four pieces of foam were put back onto the safety frame and the foam was covered by sheets. Eyelets and washers were used to hold the foam in place (Figure 3.8a) and a narrow wood plate was put at the bottom of each piece of foam (Figure 3.8b).

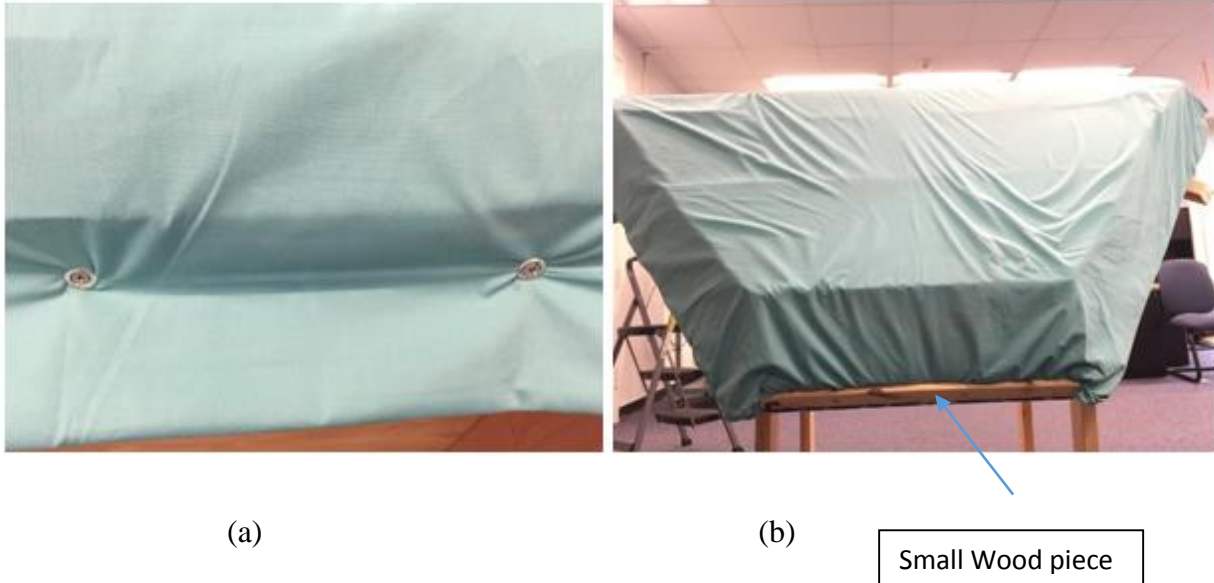


Figure 3.8: (a) Using eyelets to hold the foam; (b) Using small wood piece to hold the foam

To provide good safety for the test subject, grip tape and foam tape were purchased. The grip tape was used on each side of the pivot plate, so that it is not too slippery to climb on the chair for the test subject (Figure 3.9). The foam tape was used to prevent the subject from getting hurt by the sharp edges or tips (Figure 3.10).

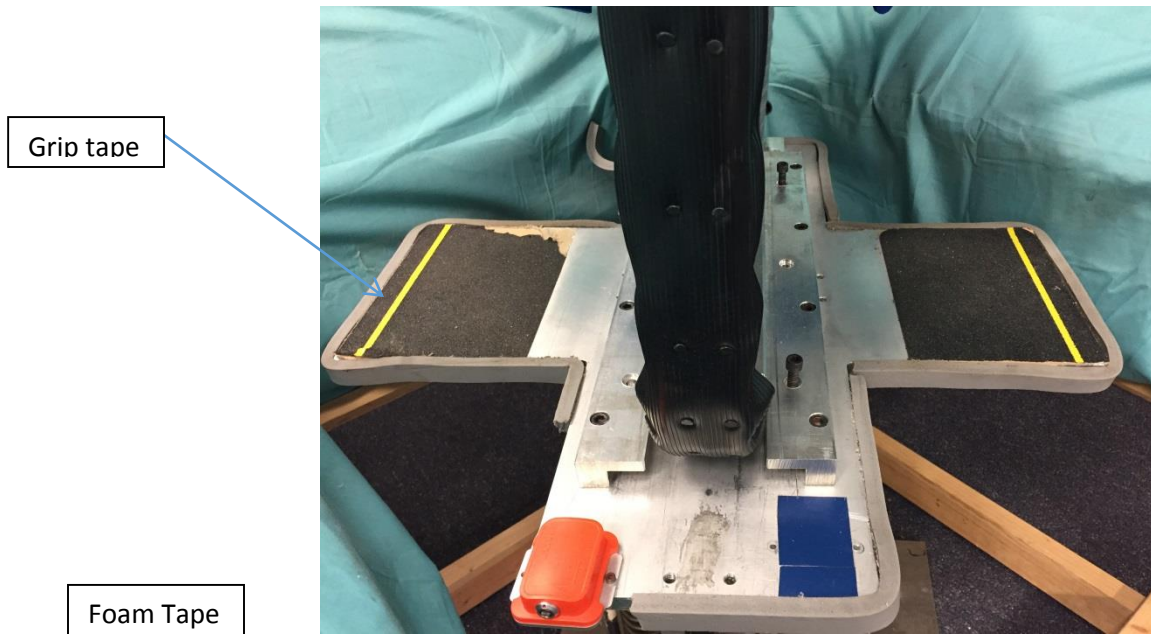
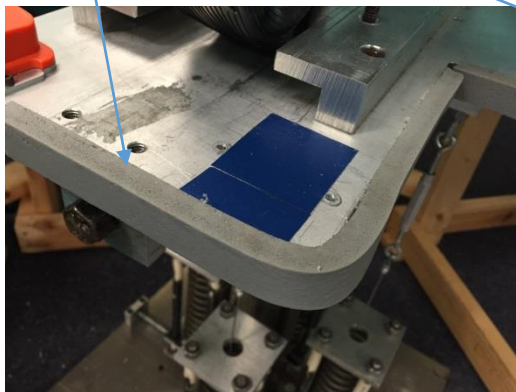


Figure 3.9: Grip tape



(a)



(b)

Figure 3.10: (a) Foam tape for sharp edge; (b) Foam tape for sharp tip

Finally, a customized LabView program was created for data acquisition from the gyroscopic sensor because the format of the data generated by the vendor's software could not be directly imported to Matlab. With the customized LabView program, data was obtained in (.txt) format, and imported to Matlab for analysis. After optimizing and calibrating the Labview

program, it became a useful tool for this research and other research in the future. The revised LabView program is showing in Figure 3.11 and Figure 3.12.

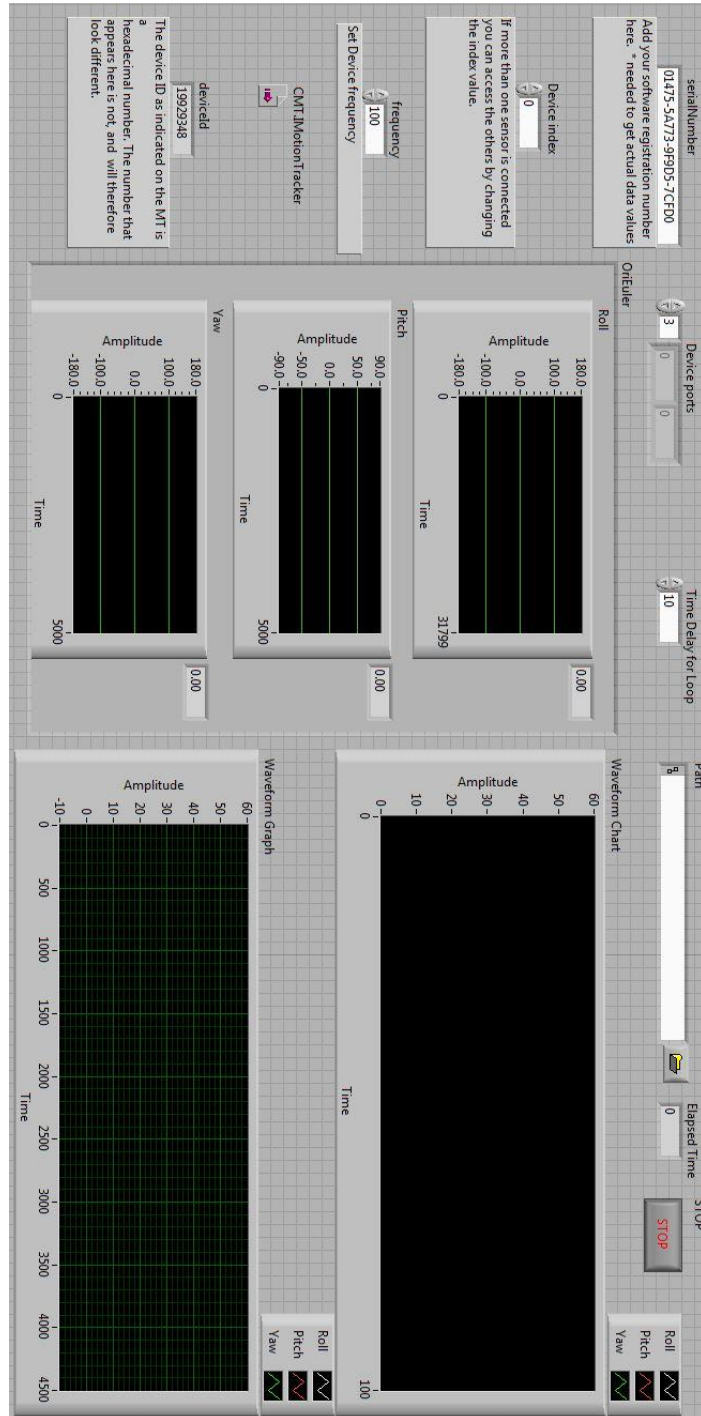


Figure 3.11: Front panel of custom LabView program

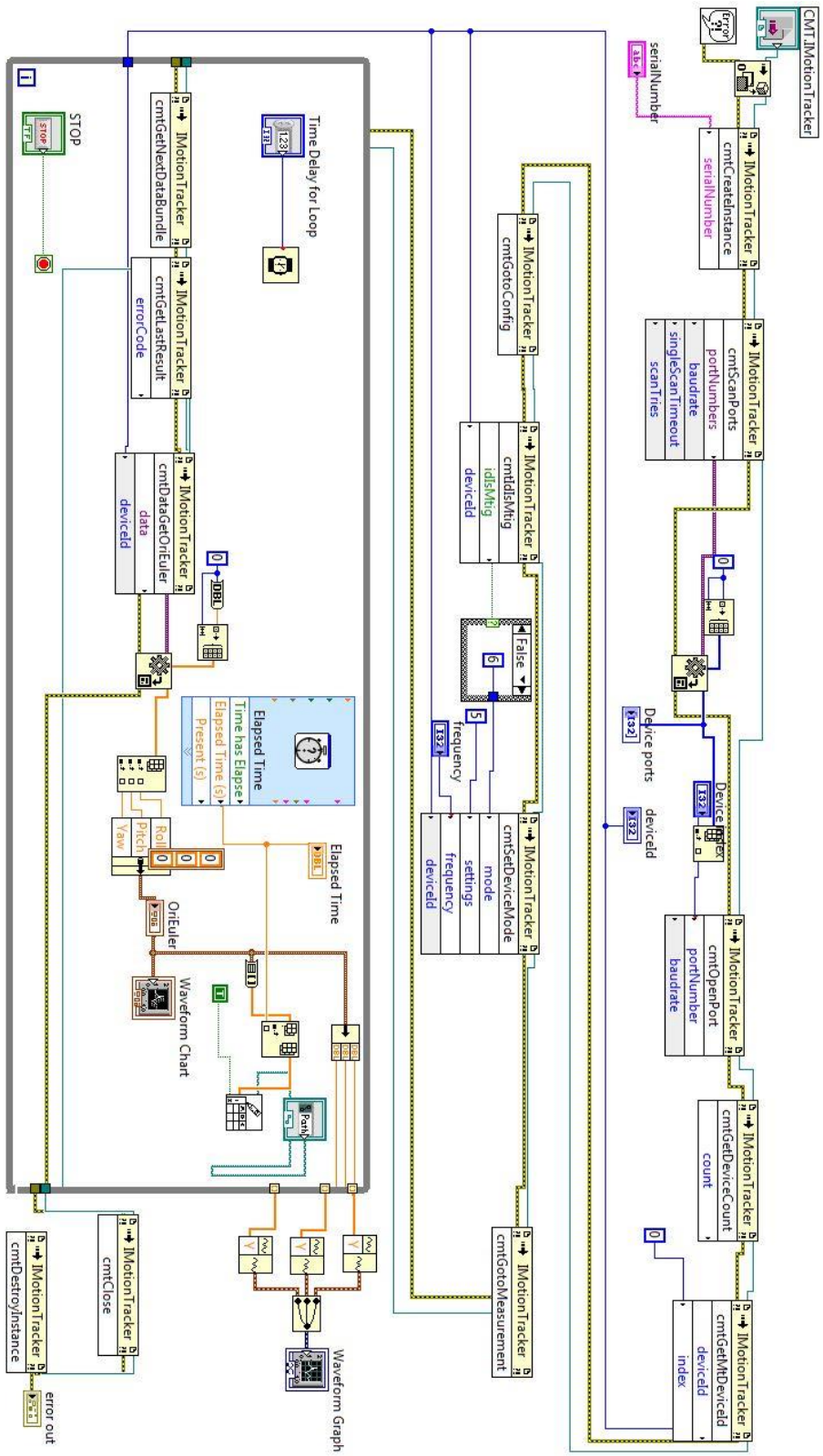


Figure 3.12: Block diagram of custom LabView program

In the LabView program, the waveform chart is used to view the data as it is being acquired during the experiment. The waveform graph is used to view the entire data set after each trial is completed. The "write to spreadsheet file" function saves the data to the designated file in (.txt) format.

3.3 Conducting The Test

3.3.1 Objective of Torso Stability Experiment

Torso stability experiment was performed to evaluate the ability of a person to maintain balance while kneeling on the BoS chair. Test subjects were asked to kneel on the BoS chair and then maintain balance with their arms crossed at the chest. The gyroscopic sensor was connected to the BoS chair and computer. The data collected using the customized LabView program was used for human torso stability analysis.

3.3.2 Test Subjects

The Institutional Review Board (IRB) training was completed by all investigators and the study was approved by the IRB. In this study, two subjects were recruited from students in Master of Science in Technology program, one male and one female. Some restrictions were placed on the age, weight, physical condition of the subject. The subject was required to be young, healthy, and have no LBP in their medical history. They were also asked to provide their age, weight and height. The subjects' information are listed in Table 3.1.

Table 3.1: The basic information of test subjects

# of subject	Gender	Age	Weight (kg)	Height (cm)
1	M	24	64.9	172
2	F	27	63.5	170

3.3.3 Preliminary Test

The preliminary test was conducted to calibrate the testing device and identify possible flaws in the testing protocol. The data collected in preliminary test was used for a pilot study. First the test protocol was created by referring to the one created by a previous WCU student [17]. The proposed test protocol was evaluated and optimized as needed. Next, the first test subject was recruited to perform the preliminary test. The subject was allowed to fall several times to become comfortable to the device, then the adjustments were made to device based on the feedbacks of the test subject. The extra foam cushion was offered for more comfort if needed. Figure 3.13a, shows the test subject kneeling on the BoS chair and holding the support rope to maintain balance. Figure 3.13b shows the test subject maintaining balance with arms crossed at the chest and hands on the shoulders. The test subject is shown falling after loss balance in Figure 3.13c.



(a)



(b)



(c)

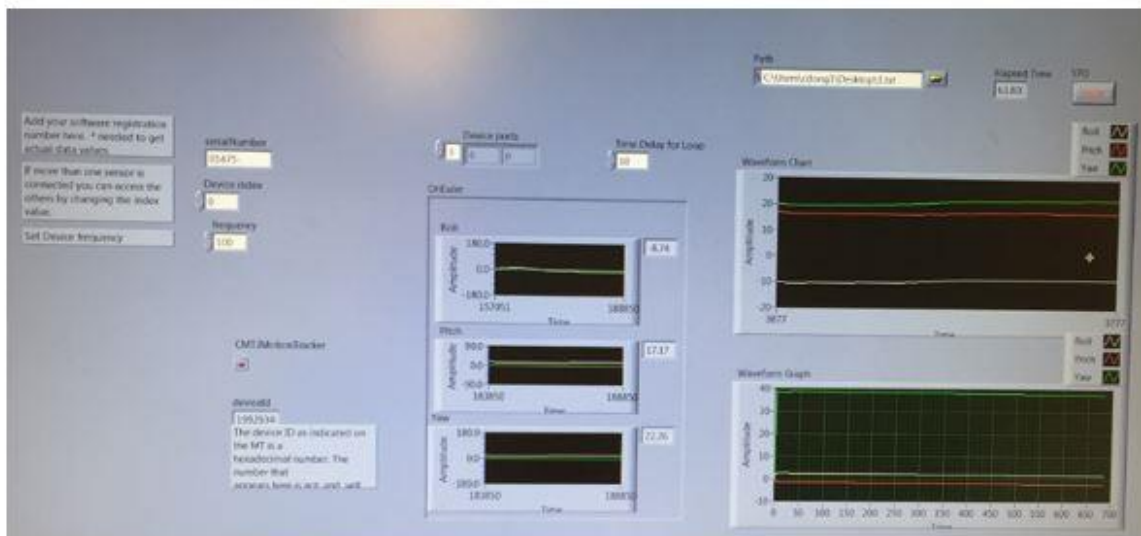
Figure 3.13: (a) The subject held the rope to keep balance. (b) The subject kept balance with arm crossed. (c) The subject fell

After these initial trials, a complete version of protocol (see Figure 3.14 and 3.15) was created. The test protocol includes each individual step needed to conduct the torso stability test and it was followed during the test. This made sure that each test was conducted in the same order, and data collected was consistent. Reducing the variations in the protocol helps to improve the accuracy of the result.

Basin of Stability Test Protocol

Before the arrival of any test subject

- Print out BoS testing sheets.
- Create a folder for each participant, and also create some blank .txt file for each trial by trial number.
- Set the chair to appropriate difficulty mode using adjustment tool (95% difficult level used for this test).
- Mount the Xsens gyrosopic sensor under the chair and then connect it with computer.
- Open customized LabView program, fill out the blank box, and choose the path for data saving. After clicking run button, it will automatically detect the Xsens device, displaying what is shown in Figure below. From three separated charts (left) and waveform chart (upper right), we can monitor the live feedback from the sensor at all times. The waveform graph (lower right) will show us the dynamical change for one complete trial.



Example of LabView code showing data readouts

Test Set-up

- Tell test subject the process, the risk involved and what to do in the test, and then ask them sign an informed consent form approved by the Institutional Review Board at Western Carolina University.
- Instruct the test subject to climb on the chair with the recommended method, which will be demonstrated if needed.

Figure 3.14: Basin of stability test protocol

- Ask the test subject to hold the support rope from above to remain stable when the test subject is seated.
- Secure the safety frame.
- Ask the test subject to cross their arms at chest-height with hands resting on the shoulders.
- Pulled away the rope from the testing area.
- Ask the test subject to concentrate by looking straight forward at an object or point on the wall and begin trying to balance.
- Allow test subject to fall a few times to become comfortable with the BoS Chair, prior to data collection.
- Offer extra cushions for more comfort if needed.
- Test subject will be able to use the rope to correct their posture as it is lowered to within their reach after each fall. The test subject can regain stability and assume the recognized balancing position with arms crossed and hands on shoulders.

Test-in-progress

- Ask the test subject to balance. If the test subject falls, the rope will be lowered so the participant could stabilize and rest, and the time will be stopped by clicking "stop" button in LabView.
- The lab assistant will await instruction to start recording, as the test subject begins to balance.
- The instant that the participant appeared to be stable, the lab assistant will be silently signaled to left click the "run" button in the LabView.
- Everyone remain quiet when the trial runs.
- Collect data, and make some notes according to subject's feedback.
- When subject falls, give the support rope to him/her. Meanwhile click the stop button in LabView, so that the data will be automatically saved.
- Follow the same procedure above and rerun the test up to ten time for same subject.

Note: The reason that data collection will be not started until the participant is stable is to obtain consistent data. If the start and stop portions of the trial are included in the recorded data, false movements would be recorded in the transition from stable to unstable. In other words, it will take a moment for the participant to attain the natural state of balance that we want to analyze.

After Test

- Notify the test subject that the test is completely finished, and give him/her the support rope.
- Promptly assist the test subject down from the chair for rest.
- Adjust chair if needed and set up the computer for data recording of next subject.

Figure 3.15: Basin of stability test protocol (continue)

3.3.4 Full Scale Test

Final tests began after development of the test protocol was completed. Each testing session consisted of ten trials for each subject. Subjects were allowed to take a rest after 5 trials if needed. Before the test subject arrived, some test preparations were made. The preparations included creating blank .txt files for data recording, connecting the gyroscopic sensor with the computer, and running a test without a subject to check if the frequencies in data were stable.

Upon arrival each subject was told the nature of test, the whole procedure and the risks involved in this test. Then the subjects were asked to sign the informed consent form approved by the IRB of WCU. The subject was then instructed to climb on the BoS chair using the step stool. When the subject was seated he/she was instructed to hold the support rope to maintain stability while the safety frames were secured. Then the subject was asked to cross his/her arms at chest height with hands resting on the shoulders and to keep balance while the support rope was pulled away.

Once the setup was finished, the first trial of the stability test was started immediately to avoid the subject fatigue. The moment that the subject indicated that he/she was ready to maintain balance, the "run" button in the LabView was clicked, and data was recorded. After the subject fell, the timer for data collecting was stopped, and the support rope was offered to the subject. The same test procedure was repeated for the same subject multiple times.

Testing sheets (see Figure 3.16) were used to record test results and take notes about test subjects' behavior during the test. The purpose of these test sheets was to help understanding

how the subject reacted when they were beginning to lose stability or lost stability during the test. The first part of the testing sheet was filled out before the test arrival which included basic information about the test subject. The table following the first part was used during the test by the investigator. The direction that the test subject fell, the time subject spent from the beginning of the test to fall, and the behavior and reaction of the test subject during the test were recorded.

Basin of Stability Testing Sheet

Difficult level:

Date:

Name:

Age:

Weight: ___ lbs. (220 lbs. maximum)

Height: ___ ft. ___ in.

Sex:

Participant #:

Data recording:

- Create a folder for each participant by participant number.

Folder Name: _____ (Participant ##)

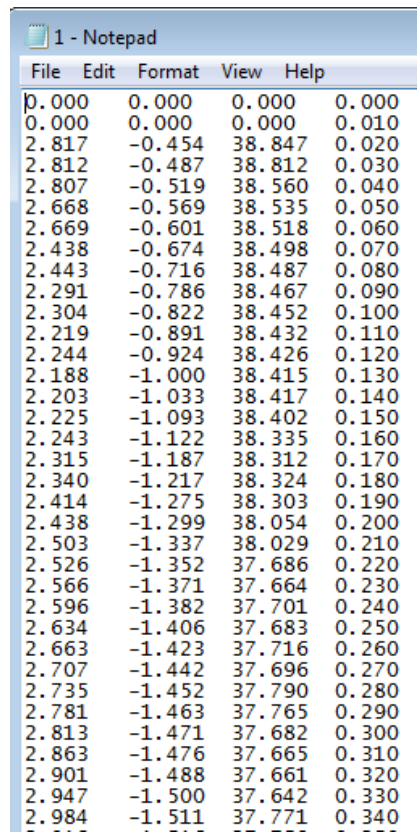
- Run trials until the subject falls.

Trial	File Name	Notes
1		
2		
3		
4		
5		
6		
7		
8		
9		
10		
11		
12		

Figure 3.16: Testing sheet

3.4 Data Collection

Two subjects with no history of LBP participated in the study. The difficulty level was set at 95%, which means that the distance between springs and the center of chair is 5% of the total distance that the spring could travel. The springs under the BoS chair are able to move 6.5 inches toward or away from the center [17]. The closer the spring is toward the center, the more difficulty the subject has maintaining balance. During the test the subject was seated on the BoS chair, and he/she had to use neuromuscular control and small dynamic movements of torso to keep a stable upright posture. The test subject on the BoS chair exhibited both stable recovery and loss of stability (falling). The angles of movements were automatically collected at a frequency of 100 Hz using the gyroscopic sensor and the customized LabView program in (.txt) format. The raw data is shown in Figure 3.17:



File	Edit	Format	View	Help
0.000	0.000	0.000	0.000	0.000
0.000	0.000	0.000	0.000	0.010
2.817	-0.454	38.847	0.020	
2.812	-0.487	38.812	0.030	
2.807	-0.519	38.560	0.040	
2.668	-0.569	38.535	0.050	
2.669	-0.601	38.518	0.060	
2.438	-0.674	38.498	0.070	
2.443	-0.716	38.487	0.080	
2.291	-0.786	38.467	0.090	
2.304	-0.822	38.452	0.100	
2.219	-0.891	38.432	0.110	
2.244	-0.924	38.426	0.120	
2.188	-1.000	38.415	0.130	
2.203	-1.033	38.417	0.140	
2.225	-1.093	38.402	0.150	
2.243	-1.122	38.335	0.160	
2.315	-1.187	38.312	0.170	
2.340	-1.217	38.324	0.180	
2.414	-1.275	38.303	0.190	
2.438	-1.299	38.054	0.200	
2.503	-1.337	38.029	0.210	
2.526	-1.352	37.686	0.220	
2.566	-1.371	37.664	0.230	
2.596	-1.382	37.701	0.240	
2.634	-1.406	37.683	0.250	
2.663	-1.423	37.716	0.260	
2.707	-1.442	37.696	0.270	
2.735	-1.452	37.790	0.280	
2.781	-1.463	37.765	0.290	
2.813	-1.471	37.682	0.300	
2.863	-1.476	37.665	0.310	
2.901	-1.488	37.661	0.320	
2.947	-1.500	37.642	0.330	
2.984	-1.511	37.771	0.340	

Figure 3.17: Raw data collected from LabView

In Figure 3.17, the data in each column represents the angle of roll, pitch, and yaw in degrees, and time in seconds, respectively. The change in pitch angle over time was analyzed in this research.

3.5 Data Analysis

Tanaka and Ross demonstrated how to analyze the time series data obtained from a mathematical model using the nearest neighbor method [13]. The same method was used in this thesis to calculate the maximum finite time Lyapunov exponent. Here after this will simply be referred to as the Lyapunov exponent. As stated in the research plan, a Matlab program was created and used to analyze the data collected from the preliminary test to make sure that the Lyapunov exponent could be calculated from the recorded data. After this was shown to be successful, this customized Matlab program was utilized to analyze the data from full scale tests. The procedure to calculate the Lyapunov exponent is outlined as below:

1. Angular velocity $\dot{\theta}$ was calculated from the derivative of angle θ with respect to time;
2. Two dimensional state space was generated, $q(t) = [\theta, \dot{\theta}]$.
3. The first 5 seconds data was removed for the male subject and first 6 seconds for the female subject.
4. The state vector was filtered using a seventh order low pass Butterworth filter at a cutoff frequency 3.2 Hz to reduce noise
5. For each trial, the first point was identified as the reference point, and all the other points represent the position of reference point evolve at time t .
6. The nearest neighbor for the reference point was obtained by calculating the Euclidian distance between the reference point and each data point from all the other trials, then

finding the data point which has the smallest Euclidean distance to the reference point using "find" function in Matlab. The points that are highly correlated with the reference point were excluded by finding the nearest neighbor in all the other trials.

7. The reference point and its nearest neighbor were evolved over the given evolution time. As the time flows toward the given evolution time, both the reference point and its nearest neighbor move forward forming two trajectories.
8. Using the method developed by Rosenstein et al. [37], and according to the definition of the Lyapunov exponent (Eq. 2.3), the maximum Lyapunov exponent is estimated by averaging the slopes of the natural logarithm of $\frac{d(\Delta t)}{d(0)}$ with respect to the evolution time Δt using "polyfit" function in Matlab.
9. Step 5-7 is repeated for all other points in one trial which are considered as the reference point.

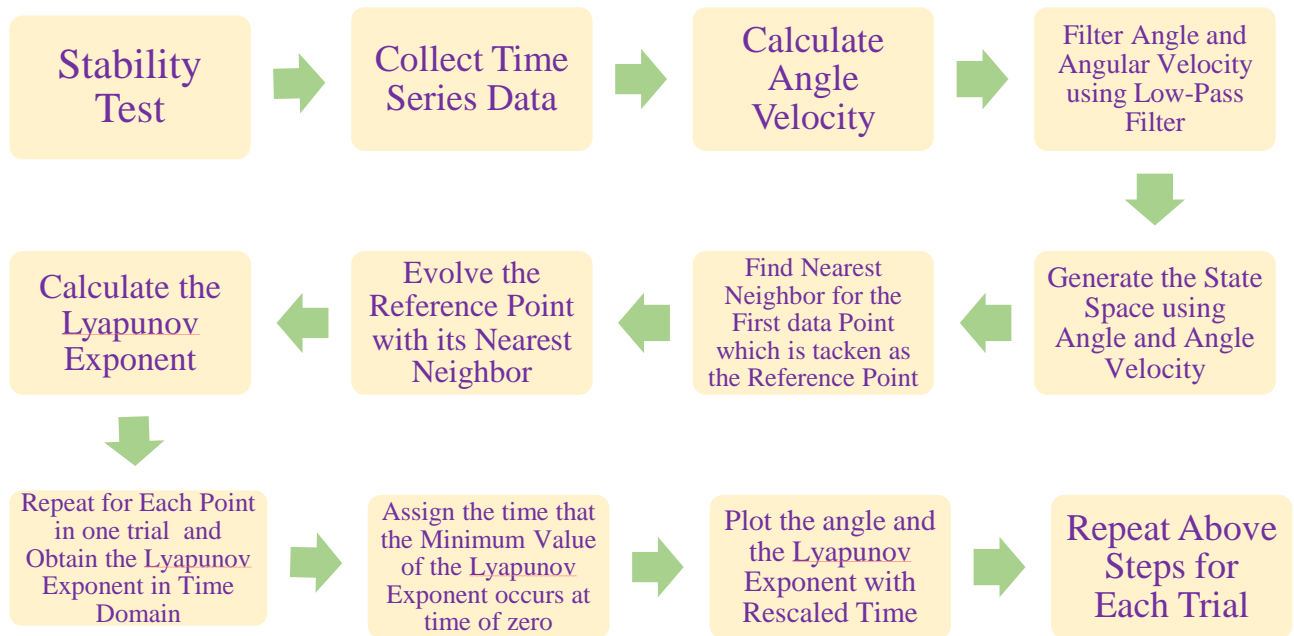


Figure 3.18: Flow chart depicting how the FTLE is calculated and plotted

CHAPTER 4: RESULTS AND DISCUSSION

4.1 Analysis and Results of Preliminary Data

The goal of this research is to record movement during the stability test using the BoS chair and to determine how the maximum FTLE changes over time. Before conducting full scale tests, it is necessary to evaluate whether the device has good performance and the data collected meets our expectations, so the preliminary test was conducted. In the preliminary test, the experiment was run and the data was collected. Measured data included the pitch angles in degree and time in second. The "diff" function in Matlab was used to calculate the angular velocity (deg/s) from the measured angular displacements. The entire data set was filtered with a 7th order Butterworth low-pass filter with a cutoff frequency of 3.2 Hz. This was the same technique that was applied to filter the data generated from mathematical models in previous studies [12, 13]. The low pass filter removes the high frequency noise in the data. Then, essential data analysis plots were generated in Matlab. Figure 4.1 shows how the pitch angle changes with time for 5 trials. For the plots that increase in the angle measurements after a stable angle change, they represent that the subject falls forward in a real test. By contrast, the plots that decrease in the angle measurements mean that the subject falls backward. Figure 4.2 is the state space plot that shows the relationship between angle and angular velocity. The plots with ejection to the upper right direction means that the subject falls forward, while the plots with ejection to the lower left direction means that the subject falls backward. Comparing with the theoretical results in Figure

2.7, it is apparent that the results in Figures 4.1 and Figure 4.2 are consistent with the theoretical results.

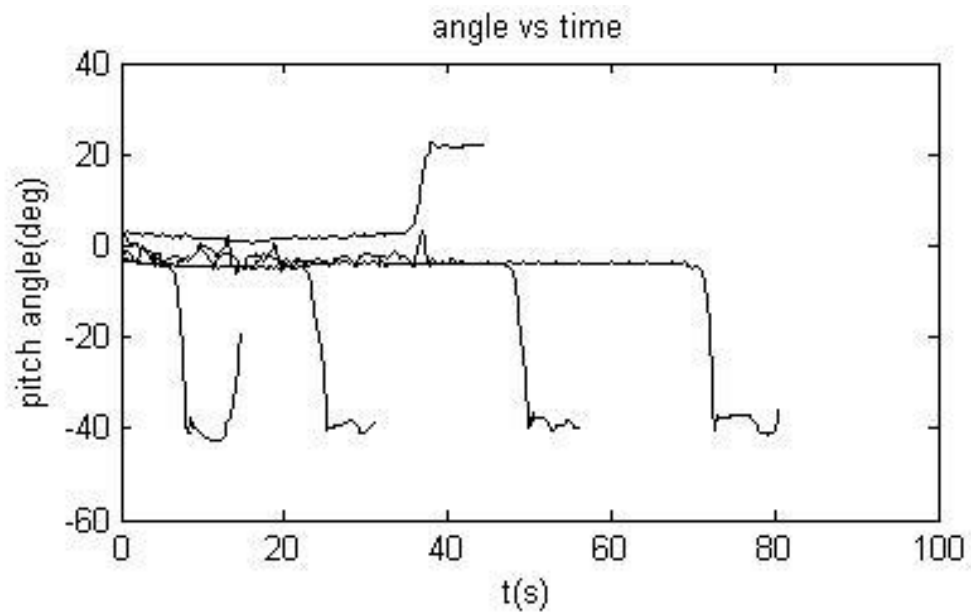


Figure 4.1: Time plots for 5 trials

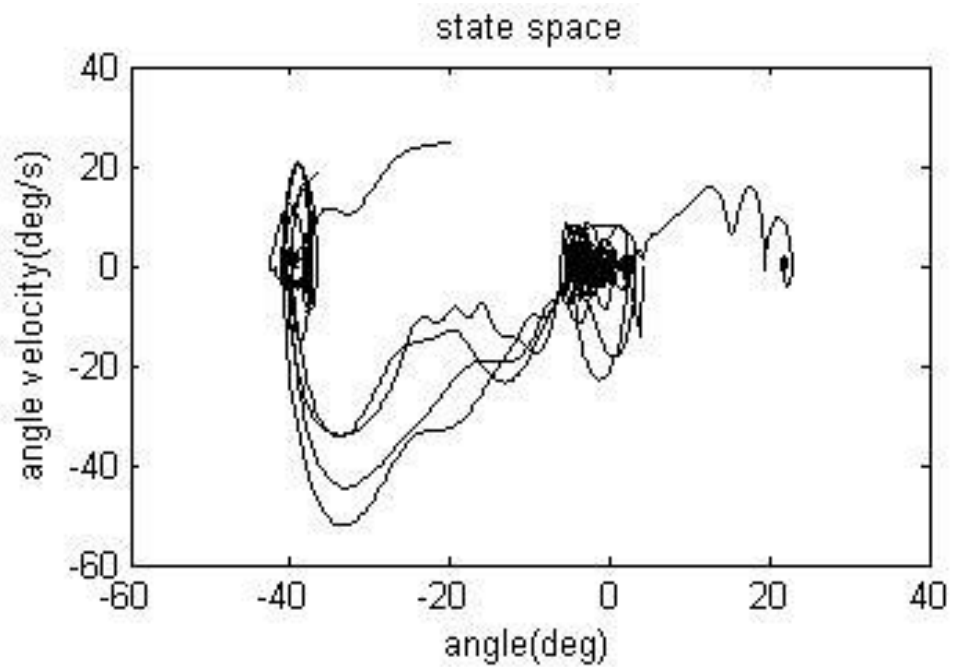


Figure 4.2: Plots in state space

Following these initial results, the analysis was continued using MATLAB. The Lyapunov exponent was calculated using different evolution times (0.05s, 0.10s and 0.15s). The magnitude of the Lyapunov exponent was observed to change when different evolution times were used (Figure 4.3). The results show that the Lyapunov exponent is sensitive to the choice of evolution time. This sensitivity will be discussed later in section 4.2.4

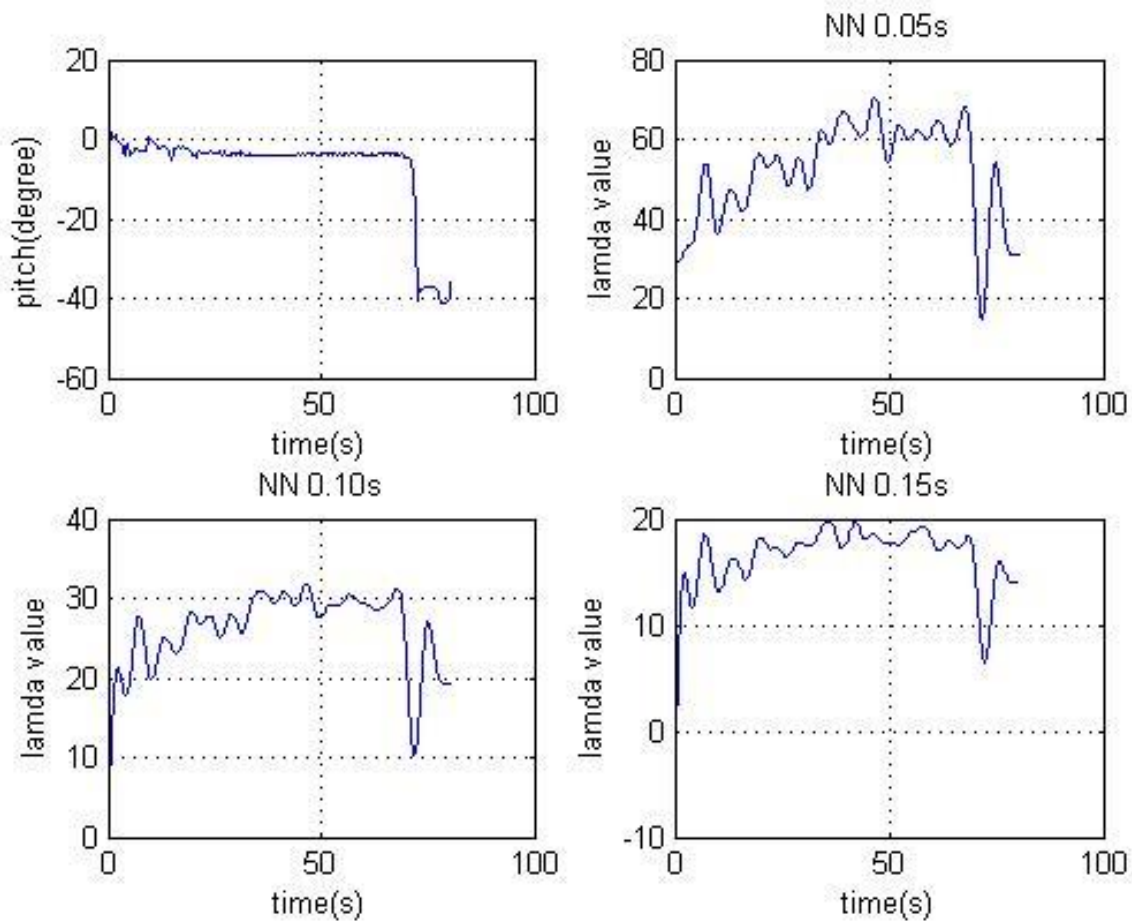


Figure 4.3: Plot of angle vs. time and Lyapunov exponent at different evolution time

For the time plot in Figure 4.1 and Figure 4.4, it was observable that the lengths of the curves are different. This is because the time length the subject maintained stability prior to falling was different in each trial. The midpoint of the fall was identified for each trial and

assigned a time of zero. The time plots were rescaled based the time of this event. Negative values indicated the number of seconds before the fall and positive values were the number of seconds after the fall. The preliminary trials were aligned based on this rescaled time line so that result from different trials can be easily compared (Figure 4.4). Then the Lyapunov exponents were calculated at each moment in time (Figure 4.4).

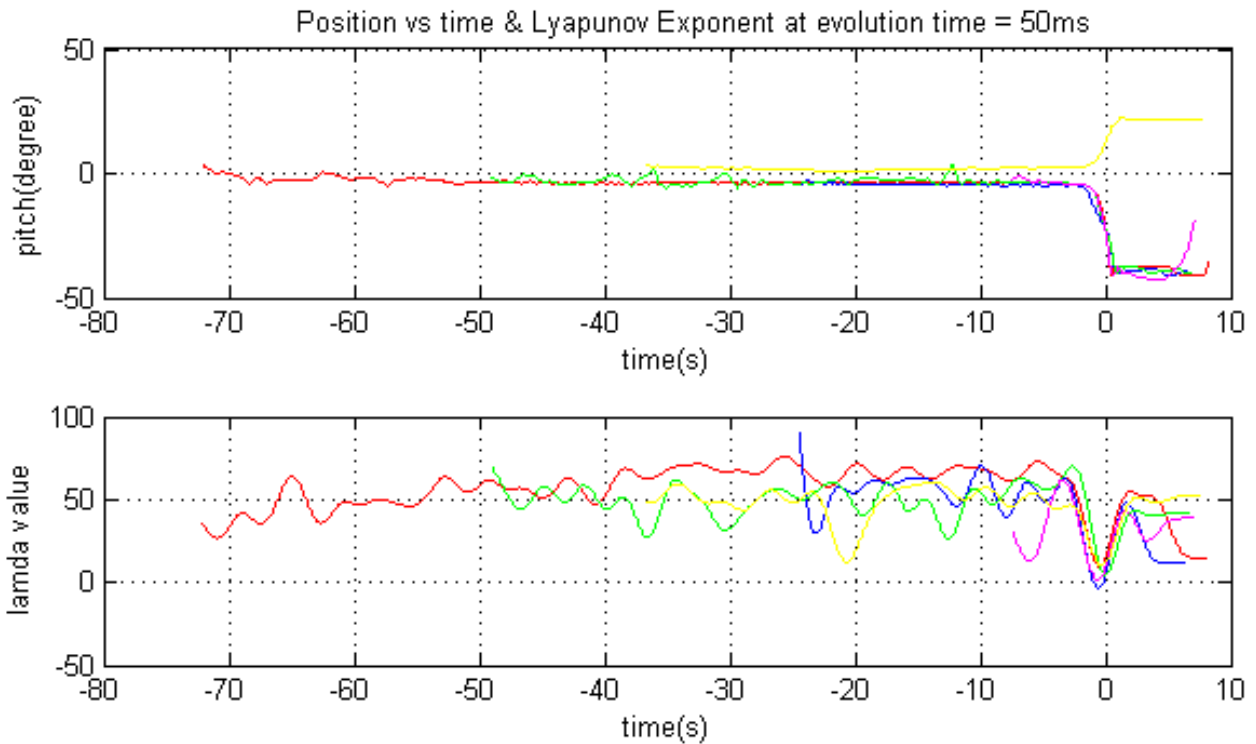


Figure 4.4: Time plots and FTLE plots in the same period

It was observed that the value of the Lyapunov exponent was associated with the value of the pitch angle at each moment in time. Before a subject falls, the value of the angle was relatively steady. Over this same time period, the Lyapunov exponent sways up and down around 50. After the subject began to fall, the angle dropped sharply to its lowest value (for backward falls; for the forward fall the angle increased). The Lyapunov exponents decreased to its

minimum value at approximately the same time. Thus, the minimum value of the Lyapunov exponent was observed to align with the falling event (zero on the timeline). After subject falls, it was noticed that the value of angle did not change much, but the Lyapunov exponent went up and then down.

The average value of the Lyapunov exponent was calculated and plotted between -6 to 5 second (Figure 4.5). The lower values of the Lyapunov exponent near time zero indicate consistent behavior of the subjects during falling. Less consistent behavior was observed prior to the fall with an average value around 45. After falling, the Lyapunov exponent was about 35. This value was between the other two and indicates that the behavior was moderately consistent after falling. In addition, it was observed that the minimum value of the Lyapunov exponent does not exactly align at zero in the timeline. The possible reason is that the middle point in the time plot was picked manually. The selection of the midpoint indicates the time of fall was somewhat arbitrary. In the later analysis, the algorithm used to rescale the time line was adjusted. The time that the minimum value of the Lyapunov exponent occurred was assigned a time of zero. The time plots and Lyapunov exponent plots were then rescaled based this value.

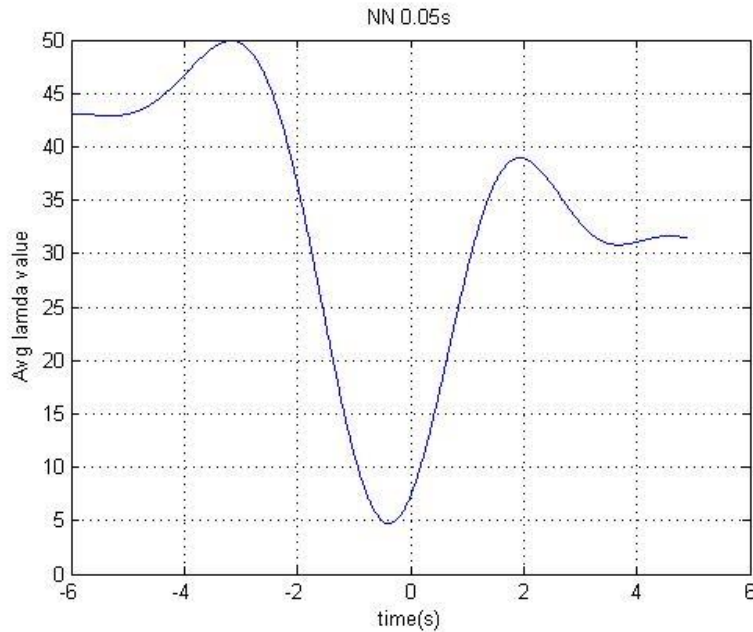


Figure 4.5: Average FTLE vs. time with evolution time 50 milliseconds

From the data analysis above, it was concluded that the data from the preliminary test met our expectations and the testing protocol and analysis methods were producing creditable data.

4. 2 Analysis and Results of Full Scale Study

For the full scale study 80 trials were completed for each of the two test subjects. The data set that showed unusual characteristics in their time plots or state space plot was not included in the analysis. The goal of the study was to identify overall behavior so anomalies were not included in determining the averages. This reduced the total number of analyzed data sets to 55 for the male subject and 60 for the female subject.

It is common to remove the data during the first few seconds of a stability test from the analysis [10, 31, 32, 40]. The reason is that the data collected during the first few seconds occurs

when the person is trying to establish stability. Data collected over this period may not accurately reflect the stability of the subject. For the male subject the data during the first 5 seconds were removed and for the female subject the first 6 seconds were removed. The amount of data cutoff for each subject was different, but this difference is not important because it occurred at the beginning of the stable period. The stable period lasts many seconds and is primarily used to establish a baseline before the critical event. Thus, no matter if the first 5 or 6 seconds of data was cut off, the remaining data still represented the stability of subjects.

4.2.1 Different Stages of Stability Test

The analysis methods developed previously were applied to the data from the full scale test. Angular velocities were calculated from the time series data. Both angles and angular velocities were filtered. All the time plots were lined up by assigning a time of zero to the time where the minimum value of the Lyapunov exponent occurred. Below are the result for the male subject (Figure 4.6).

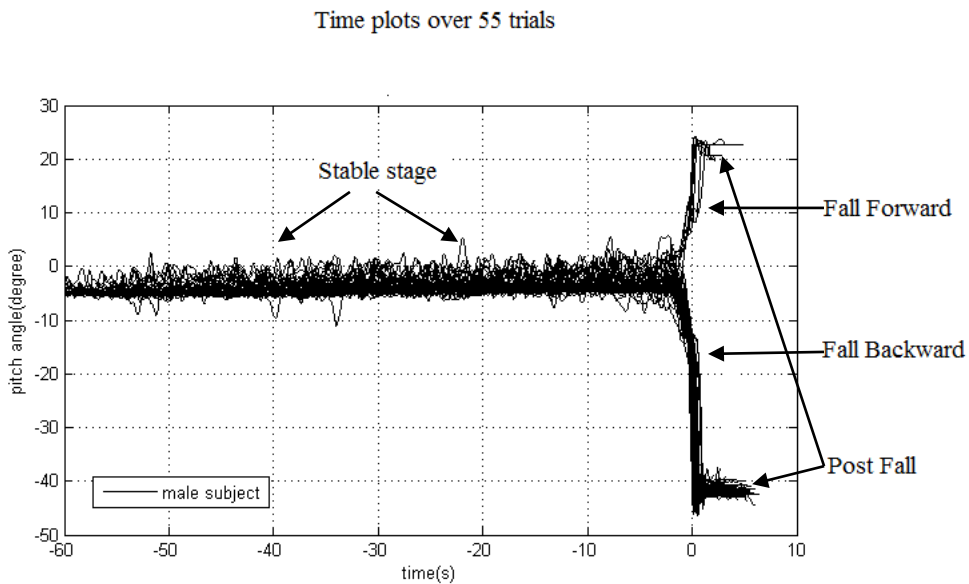


Figure 4.6: Time plot for 55 trials and lining up at $t = 0$

In Figure 4.6, it is observed that the angle remains small around zero degrees then diverges sharply up or down depending on the direction of fall. During the time prior to zero second, the subject kept balance around the equilibrium point, and this time duration is called the stable stage. It is noticed that the angle in the stable stage was below the zero line. This is because the subjects tended to balance leaning backwards at a slight angle, about 5 degrees. For conveniently visualizing the result, the time plots were centralized (Figure 4.7). The centered time plots show that the falling region lies between -40^0 and 30^0 . Compared to the falling region of $\pm 15^0$ in mathematical model (Figure 2.7), the falling region in this stability test is rather large. This large falling region allows the trajectories to be tracked for a longer time and a more complete understanding of how the Lyapunov exponent changes during falling can be obtained.

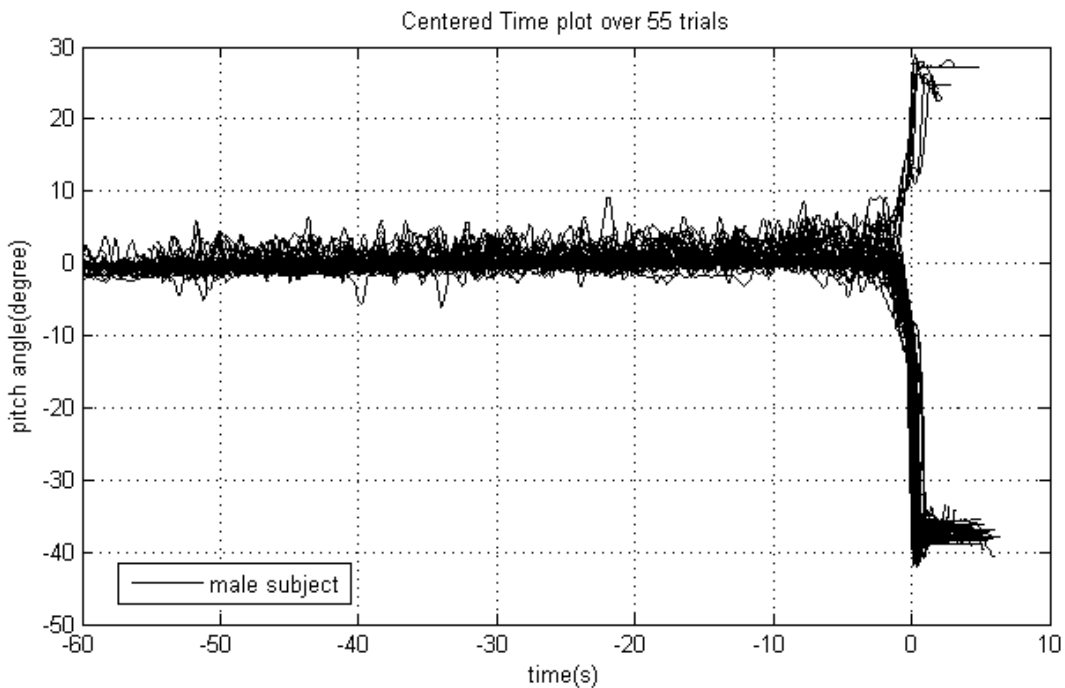


Figure 4.7: Centered time plot for 55 trials and lining up at time zero

In the state space plot (Figure 4.8), it is observed that the trajectories circle around the state space origin, (0,0). Physically, this means that the test subject kept balance near the equilibrium point. Eventually the trajectories eject to the upper right or lower left. This ejection means that subjects fell exhibiting unstable and unrecoverable behavior. The post fall characteristics can be observed in either directions of falling. When the subject hit the foam after the fall the velocity reduced to zero. All the behavior that was observed in state space was consistent with behavior observed in the time plot (Figure 4.7). In addition, Figure 4.8 shows that most trajectories are ejecting into lower left direction and just a few into upper right direction. This indicates that the number of times the subject fell backward was more than the number of times that the subject fell forward. This behavior validates the conclusion that the system seems less tolerant to perturbations in the backward direction than forward direction, as stated in the mathematical modeling study [16].

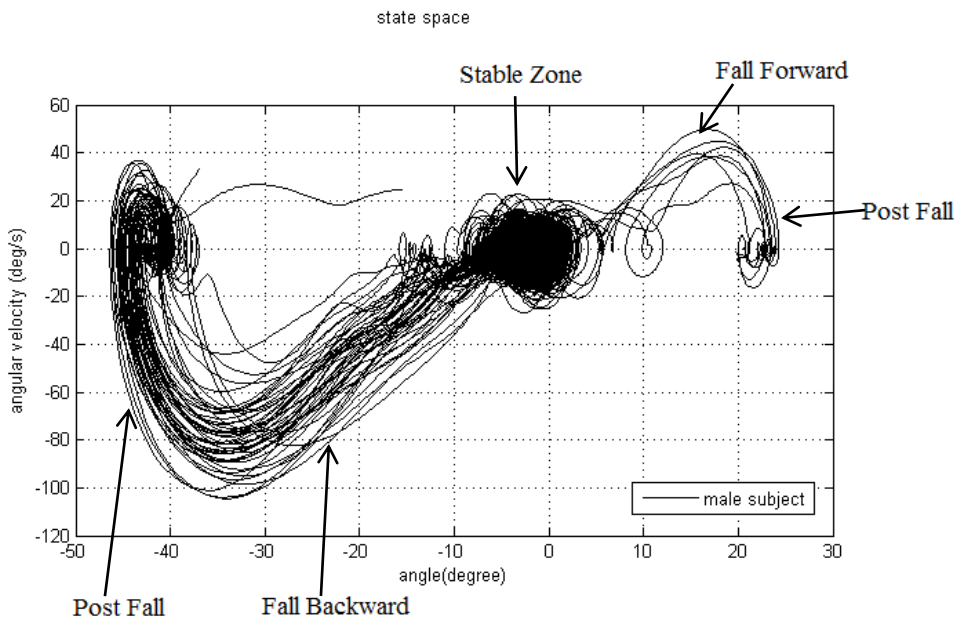


Figure 4.8: State space plot

Calculating the Lyapunov exponent for each point in the time domain provides more information about the system dynamics than only calculating a single scalar value for the Lyapunov exponent as performed in other studies [31, 32, 44]. Therefore, the averaged Lyapunov exponent in 55 trials of the same subject was calculated for each moment of time and plotted in Figure 4.9. This plot represents a complete stability test, which includes a stable stage, transition stage, falling stage, and a post fall stage. In the stable stage, it is noticed that the Lyapunov exponent sways up and down around 105, and it represents the test subject maintaining balance. He/she may fall slightly in any direction, but recovers from the perturbation and returns to the balance position using the neuromuscular control. In the transition stage, it is observable that there is a small peak. This peak may be an indicator that the test subject began to lose stability. Next is the falling stage. In this stage, it is seen that the Lyapunov exponent sharply drops from about 95 to 47, and the whole process lasts less than 2 seconds. It indicates that the test subject lost control and fell from the balancing position. The final stage is the post fall stage. After the test subject fell, he/she hit the foam of safety frame at first and then bounced off. This is why the Lyapunov exponent was observed to increase and then decrease. At this time the test subject entered another stable position resting on the foam pad. All these observations are consistent with the results that we found in time plots (Figure 4.7) and state space plots (Figure 4.8).

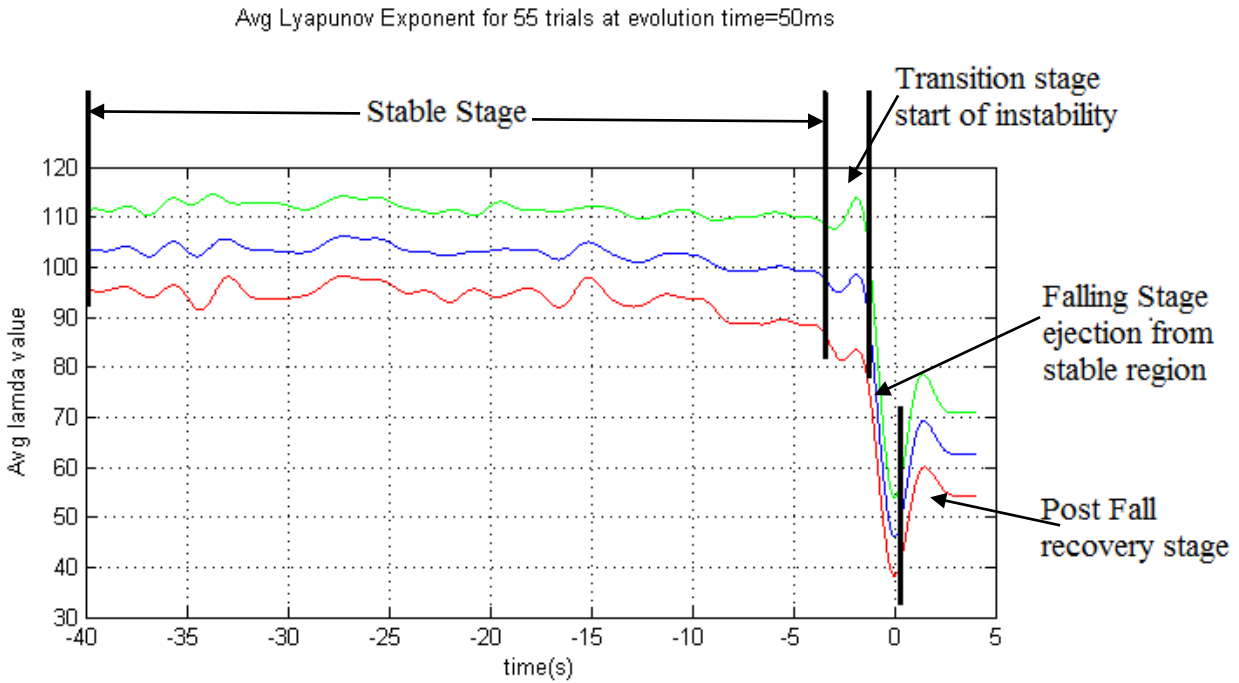


Figure 4.9: Different stages of stability test

The entry zone, the stable zone, the transition zone and the ejection zone can be observed in the state space plot (Figure 4.10). In a physical experiment, the entry zone would represent a subject lying on the foam pad and rising toward the stable zone. This type of movement is unrealistic in a physical experiment. In the stable zone the subject generally maintained an upright vertical position. Subjects move from the stable zone to the unstable zone by passing through the transition zone. In the ejection zone the subject falls away from the stable zone in an unrecoverable way.

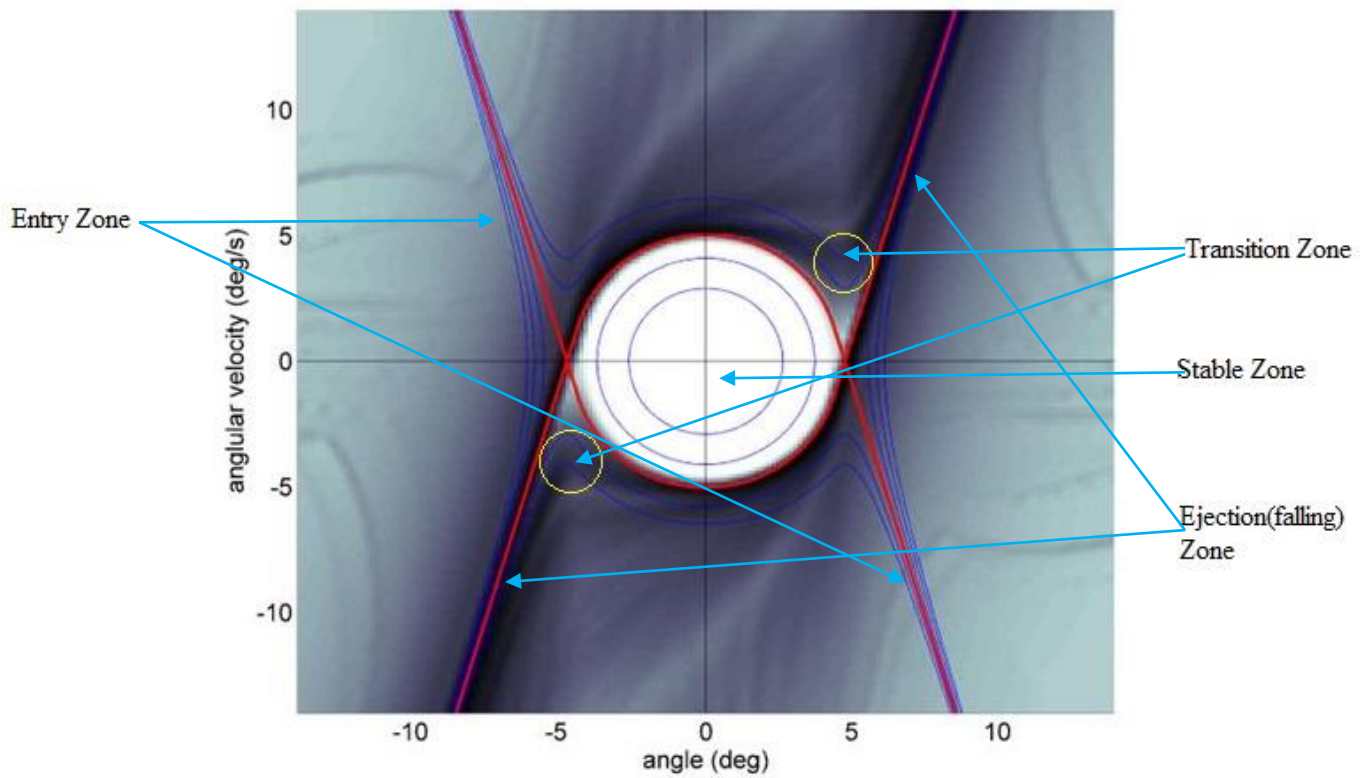


Figure 4.10: FTLE field with reverse time flow [13]

In Figure 4.11, it is seen that the three dimensional view of finite time Lyapunov exponent field has a "volcano shape". The ridges in the center separate stable motion from the unstable motion (falling). The analysis results of four different stages in the Lyapunov exponent plot (Figure 4.9) are all consistent with the results from the mathematical model (Figure 4.10 and 4.11 [13]). This indicates that the deterministic behaviors have been identified from the dynamic system in this stability test.

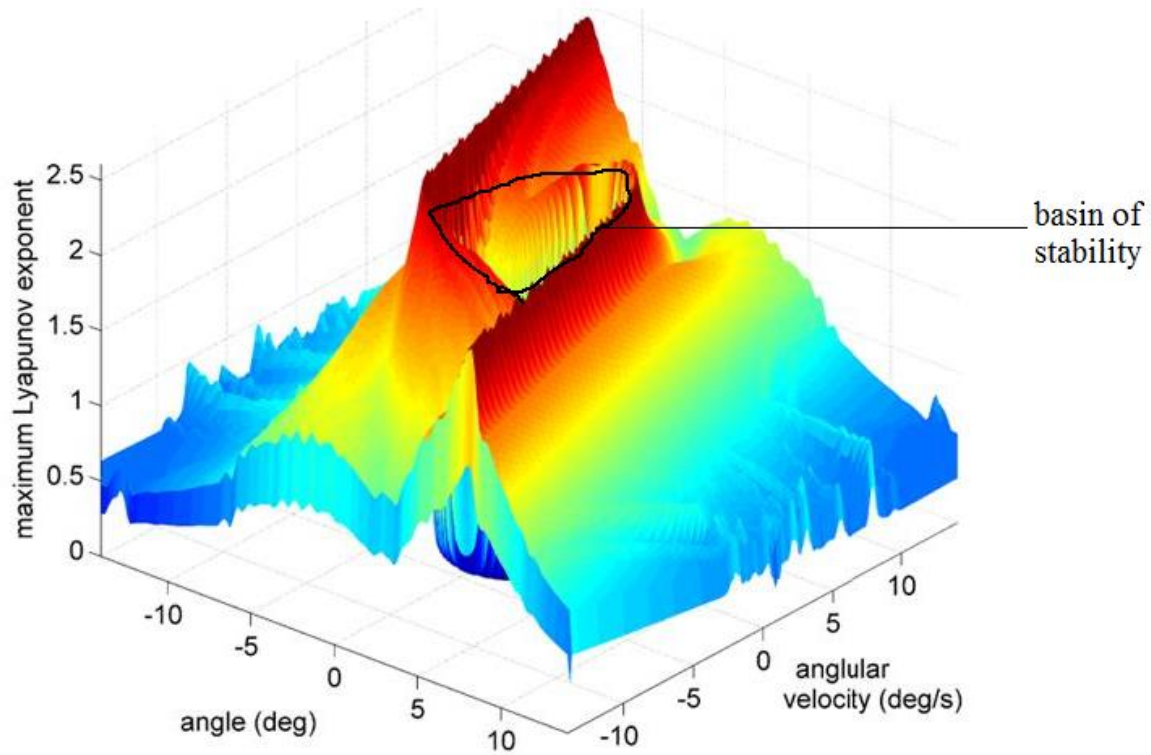


Figure 4.11: State-space-average Lyapunov exponent from mathematical model [13]

Analysis of the different stages of the stability test can help us to better understand the system dynamics. Since LBP may be caused by extreme or excessive tissue strain associated with a loss of stability, clarifying what happens in each stage of the stability test may provide useful information to evaluate the factors which cause LBP. It may lead to better prevention methods and improve treatment of spinal injuries and LBP [16].

Neuromuscular control plays an important role during the stability test. In the mathematical model of stability study, a PD controller was used to simulate human neuromuscular control [16]. However, the actual human control is much more complicated and

effective [16]. In this stability test, human subjects maintained stable behavior with neuromuscular control then fell because the neuromuscular control lacked the ability to stabilize the subject. From the analysis results, it was observed that in the steady stage movement remained within the basin of stability. Therefore, the phenomenon in the stability test and the mathematical model were consistent.

The transition zone is also very important in the stability test. A small peak was observed in the transition stage before falling, which can be a significant indicator of a future event. Take the airbag in the motor vehicle as an example. When the sensor detects the impact, the control system makes a decision to deploy the airbag which occurs only within 15 to 30 milliseconds after the onset of the crash. It will inflate rapidly for providing occupant protection and restraint during a crash [46]. So, this indicator in the transition zone could be used in the same way to avoid falling, as long as the fall can be detected and preventative action taken quickly.

4.2.2 Effect of Gender on The Lyapunov Exponent

Angular data collected from male and female subjects were analyzed in Matlab to determine if there were any differences associated with gender. However, because there was only one subject of each gender, these results will need to be further investigated in a future study with more subjects. The mean and standard deviation of the Lyapunov exponents were calculated for both male and female subjects. It was observed in Figures 4.12, and Figure 4.13 that the average Lyapunov exponent stays between ± 1 standard deviation zone for both genders.

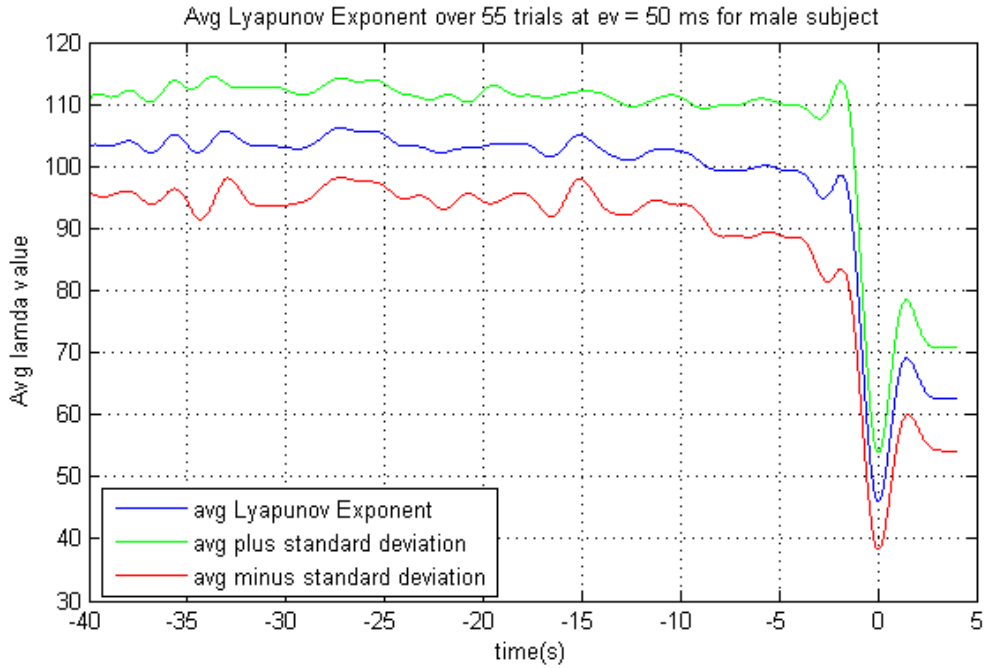


Figure 4.12: Average FTLE at evolution time 50 milliseconds for male subject

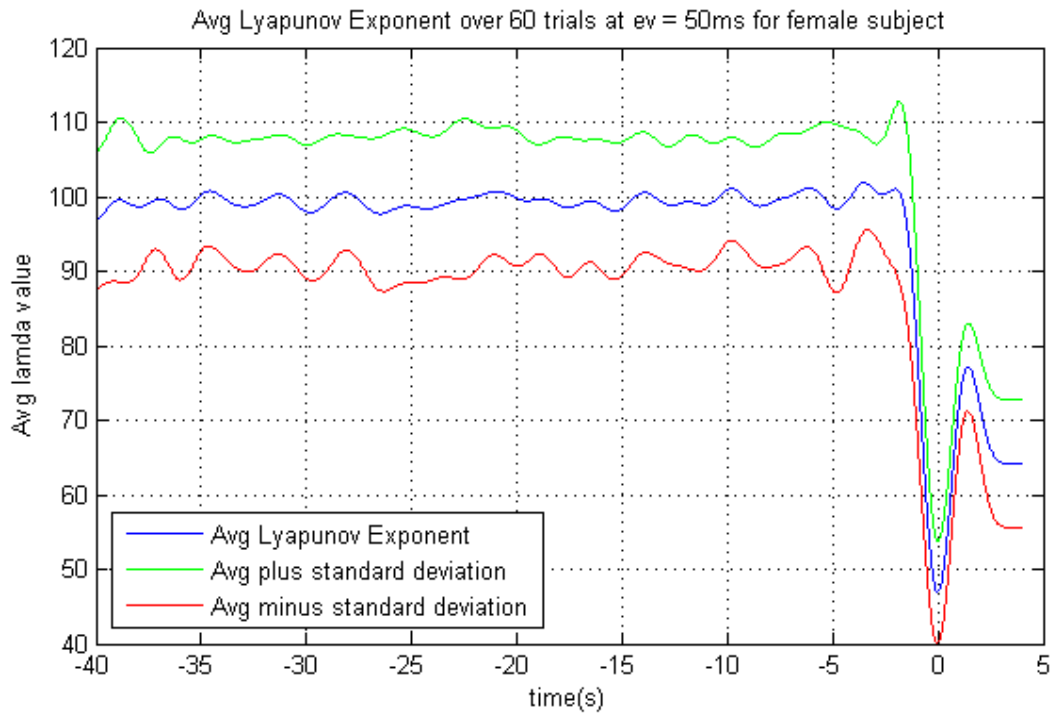


Figure 4.13: Average FTLE at evolution time 50 milliseconds for female subject

Figure 4.14 compares the Lyapunov exponent of the male to the female subject. It can be seen that the value of the Lyapunov exponent is gradually reduced before falling for the male subject, while the averaged Lyapunov exponent keeps steady before falling for the female subject. The possible reason for this is that the female subject participated in earlier stability tests and had more testing experience than the male subject. It can be seen that the Lyapunov exponent of the male subject is larger than the female subject during the first 32 seconds and the Lyapunov exponent for female subject is larger than the male subject in the following 8 seconds. The reason for this difference is unknown. It could be investigated in a future study with more test subjects. During the falling stage, the Lyapunov exponent was nearly identical for both genders. In the post fall stage, the value of the Lyapunov exponent was larger than that of the male. One possible reason for this difference was that after losing stability the male subject directly fell into the foam pad. However, the female subject often used her hands to catch herself as she neared the foam pad. As a result her behavior would be more inconsistent leading to higher Lyapunov exponents.

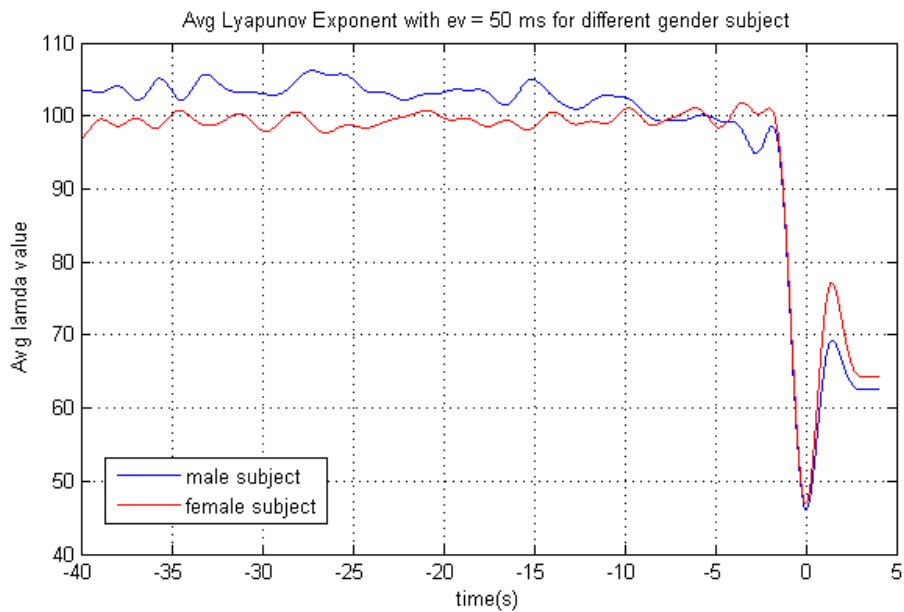


Figure 4.14: Average FTLE vs time at evolution time = 50 ms for different gender subject

Overall, the behavior observed for males and females was quite similar. However, the effect of gender on the Lyapunov exponent cannot be made due to the small number of subjects.

4.2.3 Effect of Different Filters on The Lyapunov Exponent

The data sets from the stability test were filtered using a seventh order low-pass Butterworth filter with cutoff frequency 3.2 Hz in Matlab. The Matlab function "*Butter (n, Wn, ftype)*" executes an order n digital Butterworth filter with a normalized cutoff frequency Wn . The formula for Wn is Eq. (4.1):

$$W_n = \frac{\text{cutoff_frequency} * 2}{\text{frequency of data collection}} \quad (4.1)$$

where the frequency of data collection during this research was 100 Hz and "*ftype*" is short for filter type. Typically, the filter type is a high-pass digital filter, low-pass digital filter, or order $2*n$ band-stop digital filter. The parameters of the filter include the order of the filter, the normalized cutoff frequency and the filter type. Here only the normalized cutoff frequency Wn is changed for comparison. Based on this, seven different filters were generated. The cutoff frequencies and Wn for these filters are listed in Table 4.1. Filter 2 is the one used for most of data analysis in this research.

Table 4.1: Lists of cutoff frequencies for different filters

# of filter	Cutoff frequency	Wn
Filter 1	2	0.04
Filter 2	3.2	0.064
Filter 3	4	0.08
Filter 4	5	0.10
Filter 5	6	0.12
Filter 6	7	0.14
Filter 7	8	0.16

The value of the Lyapunov exponent was compared with different filters, but same gender (male gender only), and same evolution time (50 ms). From Figure 4.15, it was observed that the value of the Lyapunov exponent increases as the cutoff frequency increases. In addition, the intervals between the fall stage and the post fall stage become narrower as the cutoff frequency increases. Furthermore, it can be seen that there is a gap between filter 1 and the other filters, and the difference among the other filters is minimal when the cutoff frequency is 3.2 Hz and above. This indicates that the Lyapunov exponent is not sensitive to the filter when the cutoff frequency is above 3.2 Hz.

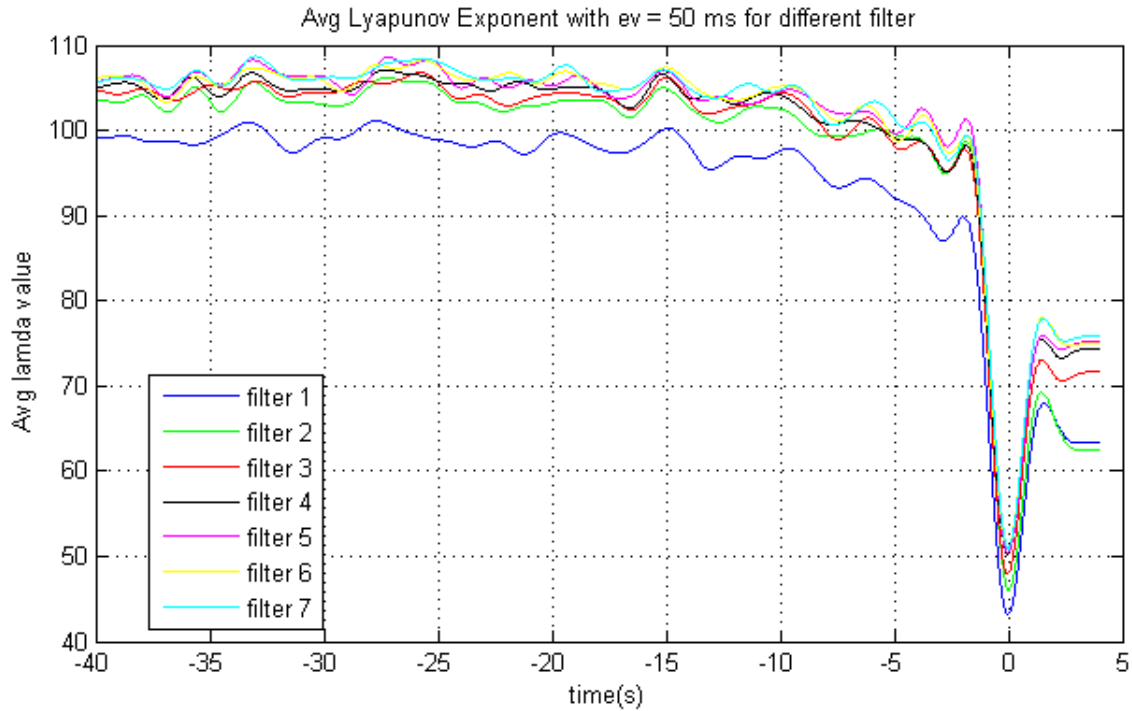


Figure 4.15: Average Lyapunov exponent plots with different filters (male, evolution time = 50 ms)

4.2.4 Effect of Different Evolution Times on The Lyapunov Exponent

The Lyapunov exponent quantifies the rate of divergence of two initially close data points. The amount of time that these two points are allowed to flow apart is the evolution time. The method used to calculate the Lyapunov exponent was taken from the research of Tanaka and Ross [13]. Based on this information, the Lyapunov exponent was calculated and plotted (Figure 4.16) for different evolution times but same gender (male subject only) and same filter (3.2 Hz).

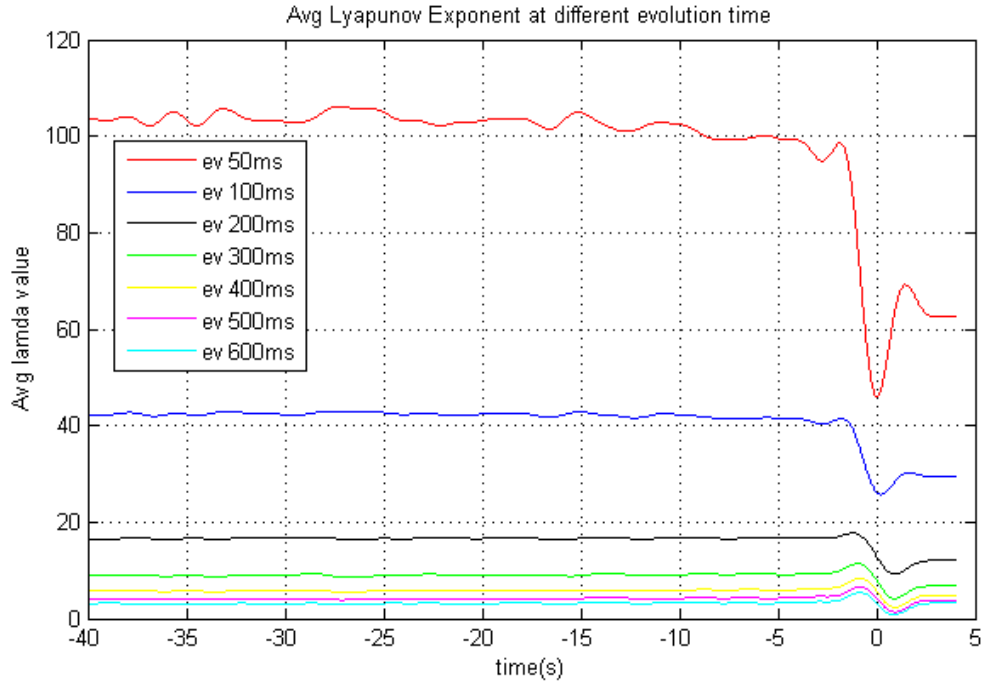


Figure 4.16: Average FTLE plots with different evolution times

From Figure 4.16 it can be clearly seen that the Lyapunov exponents decreases as the evolution time increases. This observation concludes that the Lyapunov exponent is highly sensitive to the change of evolution time. This conclusion is consistent with the algorithm of the Lyapunov exponent in the research of Wolf et al. where they created different programs to calculate Lyapunov exponents for different evolution times [36].

In order to more easily compare the results, the Lyapunov exponents was normalized to a range of 0 - 1. The formula used to normalize the Lyapunov exponent is Eq. (4.2)

$$X_{i,0 \text{ to } 1} = \frac{X_i - X_{Min}}{X_{Max} - X_{Min}} \quad (4.2)$$

where X_i is each average Lyapunov exponent i , X_{Min} is the minimum value among all average Lyapunov exponents, X_{Max} is the maximum value among all the average Lyapunov exponents, and $X_{i, 0 to 1} = \frac{X_i - X_{Min}}{X_{Max} - X_{Min}}$ is the normalized Lyapunov exponent X_i between 0 and 1.

These normalized Lyapunov exponents were plotted for different evolution times (Figure 4.17). Even in the normalized plot, the Lyapunov exponent was observed to be sensitive to changes in evolution time. In addition, it was observed that the minimum value of the Lyapunov exponent was shifting to the right of time zero as the evolution time increases. This is because zero value of time is assigned using the minimum value of the Lyapunov exponent with a 50ms evolution time. All other Lyapunov exponent plots for the other evolution times use the same time reference.

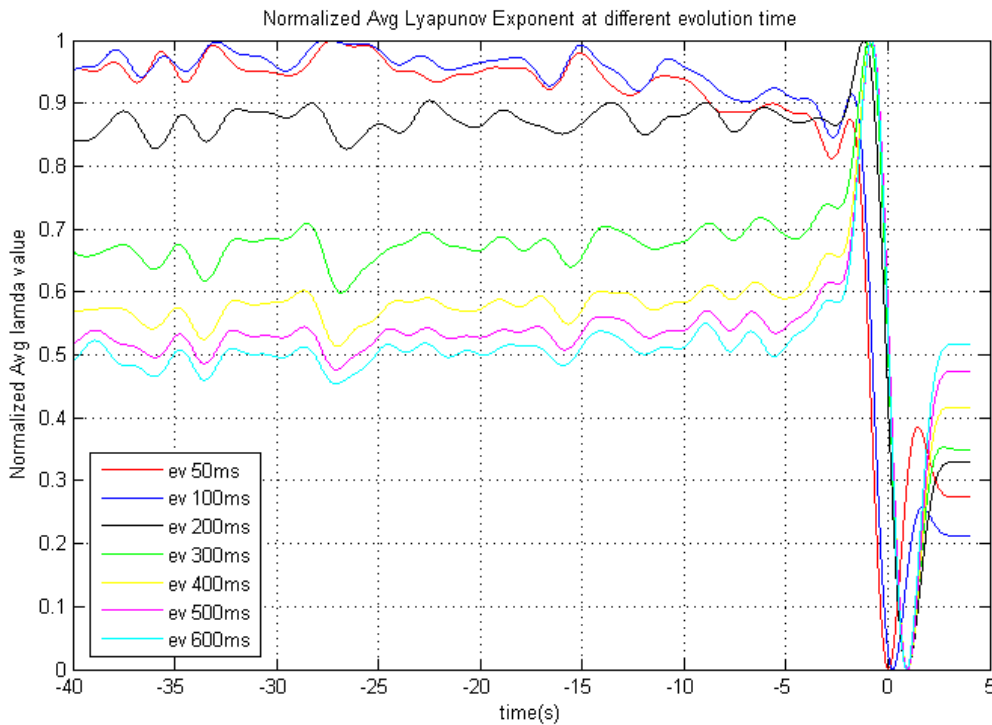


Figure 4.17: Normalized average FTLE vs time with different evolution time

CHAPTER 5: CONCLUSION AND FUTURE WORK

In this research, the BoS chair was used to measure human torso stability. Data was collected during the stability test using a gyroscopic sensor and a custom LabView program. The maximum finite time Lyapunov exponent was calculated and plotted in the time domain using Matlab. Factors that may affect the results were also investigated. The research indicated that the Lyapunov exponent was not sensitive to the cutoff frequency of the low pass filter when it was above 3.2 Hz. However, the Lyapunov exponent was sensitive to changes in evolution time.

The BoS chair allowed for large angular deflection so that the dynamics can be tracked during falling. This had never been done before for a torso stability test. By capturing these fall dynamics, the Lyapunov exponent could be calculated in the transition stage and during falling.

Another key point of this research is the study of how the Lyapunov exponent changes with time as it approaches a critical event. Previous researchers had calculated Lyapunov exponent as a single scalar value or plotted how it changes in state space. We are not aware of any other researchers who have calculated the Lyapunov exponent in the time domain. Tracking the Lyapunov exponent in the time domain may be useful as an indication to predict a future event. This approach not only can be used for this research, but is also generalizable to other dynamic systems that have critical events.

In the future studies, a test can be conducted with a larger population to confirm the results of this study and to establish a baseline for normal healthy people. This will also enable us to determine if there is a difference between genders. Torso stability of LBP patients can be measured to improve the understanding of this condition and its effect on LBP. The performance of LBP patients will be compared with non-LBP subjects to determine how they differ. Performance of patients before and after treatment could also be compared to determine whether the treatment has an effect.

BIBLIOGRAPHY

- [1] Hoy, D., Bain, C., Williams, G., et al., "A systematic review of the global prevalence of low back pain," *Arthritis & Rheumatism*, vol.64 no.6, pp. 2028-2037, 2012
- [2] F. Yao, M. L. Fontes, and V. Malhotra, *Yao & Artusio's anesthesiology: problem-oriented patient management*, 7th ed. Philadelphia: Lippincott Williams & Wilkins, 2012.
- [3] S. Taimela, U. M. Kujala, J. J. Salminen, and T. Viljanen, "The prevalence of low back pain among children and adolescents," *Spine*, vol. 22, pp. 1132–1136.
- [4] J. A. Salomon, H. Wang, M. K. Freeman, T. Vos, A. D. Flaxman, A. D. Lopez, and C. J. Murray, "Healthy life expectancy for 187 countries, 1990–2010: a systematic analysis for the global burden disease Study 2010," *The Lancet*, vol. 380 (9859), pp. 2163–2196.
- [5] G. B. Andersson, "Epidemiological features of chronic low-back pain," *The Lancet*, vol. 354(9178), pp. 581–585, 1999.
- [6] H. R. Guo, S. Tanaka, W. E. Halperin, and L. L. Cameron, "Back pain prevalence in US industry and estimates of lost workdays.," *Am J Public Health American Journal of Public Health*, vol. 89(7), pp. 1029–1035, 1999.
- [7] J. N. Katz, "Lumbar disc disorders and low-back pain: socioeconomic factors and consequences," *The Journal of Bone and Joint Surgery (American) J Bone Joint Surg Am*, vol. 88 (suppl 2), pp. 21–24, 2006.
- [8] D. I. Rubin, "Epidemiology and risk factors for spine pain," *Neurologic Clinics*, vol. 25(2), pp. 353–371, 2007.

- [9] A. Ruhe, R. Fejer, and B. Walker, "Is there a relationship between pain intensity and postural sway in patients with non-specific low back pain?" *BMC Musculoskeletal Disorders*, vol. 12, pp. 162–162, 2011.
- [10] M. L. Tanaka, M. A. Nussbaum, and S. D. Ross, "Evaluation of the threshold of stability for the human spine," *Journal of Biomechanics*, vol. 42, pp. 1017–1022, 2009.
- [11] M. L. Tanaka, K. P. Granata, "Methods & nonlinear analysis for measuring torso stability," *In ASCE 18th Engineering Mechanics Division Conference*, Blacksburg, VA, June 3–6 2007
- [12] M. L. Tanaka, S.D. Ross, "Locating separatrices and basins of stability in biodynamic systems," *Proceedings of the ASME 2008 Summer Bioengineering Conference (SBC2008)*
- [13] M. L. Tanaka, S.D. Ross, "Separatrices and basins of stability from time series data: an application to biodynamics," *Nonlinear Dynamics*, vol. 58(1), pp. 1-21, 2009.
- [14] S. D. Ross, M. L. Tanaka, and C. Senatore, "Detecting dynamical boundaries from kinematic data in biomechanics," *Chaos Chaos: An Interdisciplinary Journal of Nonlinear Science*, vol. 20 (1), pp. 017507, 2010.
- [15] M. L. Tanaka and S. D. Ross, "Using topological equivalence to discover stable control parameters in biodynamic systems," *Computer Methods in Biomechanics and Biomedical Engineering*, pp. 875–884, 2011.
- [16] M. L. Tanaka, S. D. Ross, and M. A. Nussbaum, "Mathematical modeling and simulation of seated stability," *Journal of Biomechanics*, vol. 43 (5), pp. 906–912, 2010.
- [17] D. F. Walter and M.L. Tanaka, "*Evaluation of torso stability using the basin of stability chair*," 2013

- [18] “Lower Back Pain: Read About Treatment and Symptoms,” *MedicineNet*. Available at: http://www.medicinenet.com/low_back_pain/article.htm#what_is_the_function_of_the_low_back. [Accessed: 2015].
- [19] “Low back pain,” *Wikipedia*. Available at: http://en.wikipedia.org/wiki/low_back_pain. [Accessed: 2015].
- [20] “Lower Back Pain Symptoms and Causes,” *Spine-health*. [Online]. Available at: <http://www.spine-health.com/conditions/lower-back-pain/lower-back-pain-symptoms-and-causes>. [Accessed: 2015].
- [21] M. Adams and P. Dolan, “Recent advances in lumbar spinal mechanics and their clinical significance,” *Clinical Biomechanics*, vol. 10 (1), pp. 3–19.
- [22] B. A. Casazza, “Diagnosis and treatment of acute low back pain,” *American family physician*, vol. 85 (4), pp. 343–350.
- [23] W. B. Kibler, J. Press, and A. Sciascia, “The role of core stability in athletic function,” *Sports Medicine*, vol. 36(3), pp. 189–198, 2006.
- [24] “Core Stability,” *Wikipedia*. Available at: https://en.wikipedia.org/wiki/core_stability. [Accessed: 2015].
- [25] “Brent Brookbush,” *Brent Brookbush*. Available at: <http://brentbrookbush.com/intrinsic-stabilization-subsystem/>. [Accessed: 2015].
- [26] “Introduction to Core Stability,” *Introduction to Core Stability*. Available at: <http://www.sportsinjuryclinic.net/rehabilitation-exercises/core-strengthening-stability/introduction-to-core-stability>. [Accessed: 2015].
- [27] J. Johnson, "Functional rehabilitation of low back pain with core stabilization exercises: suggestions for exercises and progressions in athletes," 2012.

- [28] K. P. Granata, G. P. Slota, and S. E. Wilson, "Influence of fatigue in neuromuscular control of spinal stability," *hfes Human Factors: The Journal of the Human Factors and Ergonomics Society*, vol. 46 (1), pp. 81–91, 2004.
- [29] M. M. Panjabi, "Clinical spinal instability and low back pain," *Journal of Electromyography and Kinesiology*, vol. 12, pp. 371–379, 2003.
- [30] J. Cholewicki, G. Polzhofer, and A. Radebold, "Postural control of trunk during unstable sitting," *Journal of Biomechanics*, vol. 33, pp. 1733–1737, 2000.
- [31] H. Lee, K. P. Granata, and M. L. Madigan, "Effects of trunk exertion force and direction on postural control of the trunk during unstable sitting," *Clinical Biomechanics*, vol. 23, pp. 505–509, 2008.
- [32] G. P. Slota, K. P. Granata, and M. L. Madigan, "Effects of seated whole-body vibration on postural control of the trunk during unstable seated balance," *Clinical Biomechanics*, vol. 23, pp. 381–386, 2008.
- [33] D. Guégan and J. Leroux, "Local Lyapunov exponents: a new way to predict chaotic systems," *Topics on Chaotic Systems - Selected Papers from CHAOS 2008 International Conference*.
- [34] G. Benettin, L. Galgani, A. Giorgilli, and J. M. Strelcyn, "Lyapunov characteristic exponents for smooth dynamical systems and for Hamiltonian systems; a method for computing all of them. Part 1: Theory," *Meccanica*, vol. 15, pp. 9–20, 1980.
- [35] I. Shimada and T. Nagashima, "A numerical approach to ergodic problem of dissipative dynamical systems," *Progress of Theoretical Physics*, vol. 61, pp. 1605–1616, 1979.
- [36] A. Wolf, J. B. Swift, H. L. Swinney, and J. A. Vastano, "Determining Lyapunov exponents from a time series," *Physica D: Nonlinear Phenomena*, vol. 16(3), pp. 285–317, 1985.

- [37] M. T. Rosenstein, J. J. Collins, and C. J. D. Luca, “A practical method for calculating largest Lyapunov exponents from small data sets,” *Physica D: Nonlinear Phenomena*, vol. 65(1-2), pp. 117–134, 1993.
- [38] J. B. Dingwell and J. P. Cusumano, “Nonlinear time series analysis of normal and pathological human walking,” *Chaos Chaos: An Interdisciplinary Journal of Nonlinear Science*, vol. 10(4), pp. 848–863, 2000.
- [39] S. A. England and K. P. Granata, “The influence of gait speed on local dynamic stability of walking,” *Gait & Posture*, vol. 25(2), pp. 172–178, 2007.
- [40] H. Lee and K. P. Granata, “Process stationarity and reliability of trunk postural stability,” *Clinical Biomechanics*, vol. 23(6), pp. 735–742, 2008.
- [41] “Dynamical System,” *Wikipedia*. http://en.wikipedia.org/wiki/dynamical_system. [Accessed: 2005].
- [42] “Math Insight,” *The idea of a dynamical system*. [Online]. Available at: http://mathinsight.org/dynamical_system_idea. [Accessed: 2015].
- [43] E. R. Scheinerman, *Invitation to dynamical systems*. Upper Saddle River, N.J.: Prentice Hall, 1996.
- [44] “Basin of attraction,” http://www.scholarpedia.org/article/basin_of_attraction. [Accessed: 2015].
- [45] “Spinal Cord Injury Facts and Figures at a Glance,” *The Journal of Spinal Cord Medicine*, pp. 68–69, 2012.
- [46] “Air Bag,” *Wikipedia*. Available at: <https://en.wikipedia.org/wiki/airbag#operation>. [Accessed: 2015]

APPENDICES

Appendix A: Main Code for How to Calculate The Lyapunov

Exponent in Time Domain

```
%%%%%%%%%%%%%%%%%%%%%%%%%%%%%%%%%%%%%%%%%%%%%%%%%%%%%%%%%%%%%%%%%%%%%%%%
%% Program for calculation the Lyapunov exponent
%%
%% Chaoke Dong
%% Original: November 4, 2014
%% Last update: October 15, 2015
%%%%%%%%%%%%%%%%%%%%%%%%%%%%%%%%%%%%%%%%%%%%%%%%%%%%%%%%%%%%%%%%%%%%%%%%

clear all
clc
tic

%%%%%%%%%%%%%%%%%%%%%%%%%%%%%%%%%%%%%%%%%%%%%%%%%%%%%%%%%%%%%%%%%%%%%%%% Import Experiment Data %%%%%%%%%
dirname = ['C:\Users\cdong1\Desktop\Research\BoS test\BOS\85
percent\Pre_test4\Data Analysis Matlab\'];
outfiledir = ['C:\Users\cdong1\Desktop\Research\BoS test\BOS\85
percent\Pre_test4\Data Analysis Matlab\'];
record_freq = 100;           % Experimental data recording at rate 100Hz
cutoff_freq = 3.2;          % Which is also filt_freq, and data is filter at
3.2 Hz
t_step = 1/record_freq;

disp('Begin Lyapunov Exponents Analysis')
disp(' ')
disp(['Input file directory name = ',dirname])
disp(['Output file directory name = ',outfiledir])
disp(' ')

%%%%%%%%%%%%%%%%%%%%%%%%%%%%%%%%%%%%%%%%%%%%%%%%%%%%%%%%%%%%%%%%%%%%%%%% Predefine a cell for storing state space vector %%%%%%%%%
qcell =cell(5,1);

%%%%%%%%%%%%%%%%%%%%%%%%%%%%%%%%%%%%%%%%%%%%%%%%%%%%%%%%%%%%%%%%%%%%%%%% Begin constructing the state space %%%%%%%%%
for s = 1:1           % Repeat for each subject
    for c = 1:1       % Repeat for each condition
        for k = 2:6   % Repeat for each trial
```

```

name = ['Working on : ', 's',int2str(s), 'c',int2str(c), 't',int2str(k)];
disp(name)
filename = ['s',int2str(s), 'c',int2str(c), 't',int2str(k), '.txt'];
disp(filename)
dat = dlmread([dirname,filename], '\t',6,0);

t = dat(:,4);           % Time (s)
pitch = dat(:,2);      % Pitch Angle (deg),also called position

%%%%%%%%%% Compute the Velocity %%%%%%%%%%%

q_v = diff(pitch)/t_step;

%%%%%%%%% Filter the angle and the velocity %%%

[b,a] = butter(7,cutoff_freq*2/record_freq,'low'); % lowpass
filter coefficients

pitch_f = filtfilt(b,a,pitch);           % Filter Angles
q_f = filtfilt(b,a,q_v);                 % Filter Velocities

%%%%%%%%%% Generate the state space%%%%%%%%%%

q = [pitch_f,[0;q_f]];                   % State = [pos, vel]
qcell{k-1} = q;

end % k
end % c
end % s

b_q = [qcell{1};qcell{2};qcell{3};qcell{4};qcell{5}];

%%%%%%%%% Calculte the Lyapunov Exponent %%%%%%%%%%%

ev = 5;%Define the evolution time is 5 time steps, which is 50 ms.
L = length(b_q)-ev+1;
L2 = length(qcell{5})-ev+1;

for ii=1:L2
rp = qcell{5}(ii,:); % reference point

%%%%%%%%% Define the range of Nearest Neighbor %%%%%%%%%%%

q2 =[qcell{1};qcell{2};qcell{3};qcell{4}(1:end-ev+1,:)];

%%%%%%%%% If statement for Finding Nearest Neighbor %%%%%%%%%%

d = zeros(length(q2),1);
for n = 1:length(d)
d(n) = sqrt((q2(n,1)-rp(1))^2+(q2(n,2)-rp(2))^2);
end
e = min(d);

```

```

[r,m]= find(d == e);
r = r;
nn = q2(r,:);

%%%%% Evolve the reference point and its nearest neighbor %%%

x1 = qcell{5}(ii:ii+ev-1,1);
y1 = qcell{5}(ii:ii+ev-1,2);
x2 = q2(r:r+ev-1,1);
y2 = q2(r:r+ev-1,2);

%%%%% calculate the distance with respect to the time
distance=zeros(1,ev);

for a=1:ev;
    distance(a)=sqrt((x1(a)-x2(a))^2+(y1(a)-y2(a))^2);
end

t_ev = 0.01:0.01:ev*0.01;%define the evolution time
d0 = distance(1);
r_distance = log(distance/d0);
r_t_ev = t_ev-t_ev(1)*ones(1,length(t_ev));%delta t
P = polyfit(r_t_ev,r_distance,1); %find the slope
lamda(ii) = P(1); %calculate the Lyapunov exponent
end %ii

index = 1:ii;
time_step = index*t_step;
[b1,a1] = butter(7,cutoff_freq*2/(10*record_freq),'low'); % lowpass filter
coefficients

lamda_f = filtfilt(b1,a1,lamda);
figure (8)
plot(time_step,lamda_f,'b');
grid on
xlabel('time(s)')
ylabel('Lyapunov exponents')
title('The Lyapunov exponent in time domain with evolution time = 50ms')
hold on

time = toc;
hours = floor(time/60/60);
mins = floor( (time-(hours*60*60))/60);
seconds = time-(hours*60*60)-(mins*60);

disp(['Time expired = ',int2str(hours),' Hours, ',int2str(mins),' Mins,
',int2str(seconds),' Seconds']);

```

Appendix B: Main Code for How to Align The Time Plots with The Lypunov Exponent Plots at Assigned Time Zero

```
%%%%%%%%%%%%%%%%%%%%%%%%%%%%%%%%%%%%%%%%%%%%%%%%%%%%%%%%%%%%%%%%%%%%%%%%
%%% Align time plot with FTLE plot at time zero
%%%
%%% Chaoke Dong
%%% Original: November 4, 2014
%%% Last update: October 15, 2015
%%%%%%%%%%%%%%%%%%%%%%%%%%%%%%%%%%%%%%%%%%%%%%%%%%%%%%%%%%%%%%%%%%%%%%%%

clear all
clc
tic

%%%%%%%%%%%%%%%%%%%%%%%%%%%%%%%%%%%%%%%%%%%%%%%%%%%%%%%%%%%%%%%%%%%%%%%% Input parameters %%%%%%%%%%%%%%%%%%%%%%%%%%%%%%%%%%%%%%%%%%%%%%%%%%%%%%%%%%%%%%%%%%%%%%%%%
dirname = ['C:\Users\cdong1\Desktop\Research\BoS test\BOS\85
percent\Pre_test4\Data Analysis Matlab\'];
outfiledir = ['C:\Users\cdong1\Desktop\Research\BoS test\BOS\85
percent\Pre_test4\Data Analysis Matlab\'];
record_freq = 100;           % Experimental data recording at rate 100Hz
cutoff_freq = 3.2;          % Which is also filt_freq, and data is filter at
3.2 Hz
t_step = 1/record_freq;
cutoff_time = 6;            %cut off first 6 seconds unsteady data
%%%%%%%%%%%%%%%%%%%%%%%%%%%%%%%%%%%%%%%%%%%%%%%%%%%%%%%%%%%%%%%%%%%%%%%%

disp('Begin Analysis')
disp(' ')
disp(['Input file directory name = ',dirname])
disp(['Output file directory name = ',outfiledir])
disp(' ')

qcell = cell(5,1);

%%%%%%%%%%%%%%%%%%%%%%%%%%%%%%%%%%%%%%%%%%%%%%%%%%%%%%%%%%%%%%%%%%%%%%%% Begin constructing the state space %%%%%%%%%%%%%%%%%%%%%%%%%%%%%%%%%%%%%%%%%%%%%%%%%%%%%%%%%%%%%%%%%%%%%%%%%

for s = 1:1                % Repeat for each subjects
    for c = 1:1            % Repeat for each condition
        for k = 2:6        % Repeat for each trial

            name = ['Working on : ', 's', int2str(s),
'c', int2str(c), 't', int2str(k)];
            disp(name)
            filename = ['s', int2str(s),
'c', int2str(c), 't', int2str(k), '.txt'];
            disp(filename)
            dat = dlmread([dirname, filename], '\t', 6, 0);

            t = dat(cutoff_time*record_freq+1:end, 4);           % Time (s)
            cutoff first 5 seconds
```

```

        pitch = dat(cutoff_time*record_freq+1:end,2);           % Pitch
Angle(deg),cutoff first 5 seconds
        q_v = diff(pitch)/t_step;           % Velocity (deg/s)

        [b,a] = butter(7,cutoff_freq*2/record_freq,'low'); % lowpass
filter coefficients
        pitch_f = filtfilt(b,a,pitch);           % filter angle
        q_f = filtfilt(b,a,q_v);           % filter Velocity

        q = [pitch_f(2:end),q_f];           % State = [pos,
vel]
        qcell{k} = q;

    end % k
end % c
end % s

%%%%%%%% Calculate the Lyapunov Exponent %%%%%%%%%%%%%%%

ev = 5; %evolution time step,50ms

for bb = 3:3
    L2 = length(qcell{bb})-ev+1;
    for ii = 1:L2
        rp = qcell{bb}(ii,:);           % reference point

        %%%%%%%%%Find the nearest neighbor%%%%%%%%%%%%%%
        q2 = [];
        for bbb = 1:5
            if bbb ~= bb
                q2 = [q2;qcell{bbb}];
            end
        end
        q21 = q2(1:end-ev+1,:);

        d = zeros(length(q21),1);

        for n = 1:length(d)
            d(n) = sqrt((q21(n,1)-rp(1))^2+(q21(n,2)-rp(2))^2);
        end
        e = min(d);
        [r,m] = find(d == e);
        nn = q2(r,:);

        %%%%%%%%%Compute the Lyapunov exponent%%%%%%%%%%%%%%
        x1 = qcell{bb}(ii:ii+ev-1,1);
        y1 = qcell{bb}(ii:ii+ev-1,2);
        x2 = q2(r:r+ev-1,1);
        y2 = q2(r:r+ev-1,2);

        distance = zeros(1,ev);

        for a = 1:ev;
            distance(a) = sqrt((x1(a)-x2(a))^2+(y1(a)-y2(a))^2);
        end
    end
end

```



```

end

t_ev = 0.01:0.01:ev*0.01;
d0 = distance(1);
r_distance = log(distance/d0);
r_t_ev = t_ev-t_ev(1)*ones(1,length(t_ev));
P = polyfit(r_t_ev,r_distance,1);
lamda(ii)=P(1);

end %ii

[b1,a1] = butter(7,cutoff_freq*2/(10*record_freq),'low');
lamda_f = filtfilt(b1,a1,lamda);
min_lamda = min(lamda_f); %find the minimum Lyapunov exponent
mid_coordinate = find(lamda_f==min_lamda);

index = 1:L2;
t_step = 1/record_freq;
time_step1 = index*t_step+(cutoff_time+1/record_freq)*ones(1,L2);
mid_point = time_step1(mid_coordinate);
time_step = time_step1-mid_point*ones(1,length(time_step1));

figure (1)
subplot(2,1,1);
plot(time_step,qcell{bb}(1:end-ev+1,1));
grid on
xlabel('time(s)')
ylabel('pitch(deg)')
hold on

subplot(2,1,2);
plot(time_step,lamda_f,'b');
grid on
xlabel('time(s)')
ylabel('lamda value')
title('NN 0.05s')
hold on

clear lamda
end %bb

time = toc;
hours = floor(time/60/60);
mins = floor( (time-(hours*60*60))/60);
seconds = time-(hours*60*60)-(mins*60);

disp(['Time expired = ',int2str(hours),' Hours, ',int2str(mins),' Mins, ',int2str(seconds),' Seconds']);

```

Appendix C: Main Code for How to Average The Lypunov Exponent

```
%%%%%%%%%%%%%%%%%%%%%%%%%%%%%%%%%%%%%%%%%%%%%%%%%%%%%%%%%%%%%%%%%%%%%%%%
%%%Calculate the average FTLE
%%%
%%% Chaoke Dong
%%% Original: November 4, 2014
%%% Last update: October 15, 2015
%%%%%%%%%%%%%%%%%%%%%%%%%%%%%%%%%%%%%%%%%%%%%%%%%%%%%%%%%%%%%%%%%%%%%%%%

clear all
clc
tic

%%%%%%%%%%%%%%%%%%%%%%%%%%%%%%%%%%%%%%%%%%%%%%%%%%%%%%%%%%%%%%%%%%%%%%%% Input parameters %%%%%%%%%
dirname = ['C:\Users\cdong1\Desktop\Research\BoS test\BOS\85
percent\Pre_test4\Data Analysis Matlab\'];
outfiledir = ['C:\Users\cdong1\Desktop\Research\BoS test\BOS\85
percent\Pre_test4\Data Analysis Matlab\'];
record_freq = 100;          % Experimental data recording at rate 100Hz
cutoff_freq = 3.2;         % Which is also filt_freq, and data is filter at
3.2 Hz
t_step = 1/record_freq;
cutoff_time = 6;          %cut off first 6 seconds unsteady data

disp('Begin Chaoke Analysis')
disp(' ')
disp(['Input file directory name = ',dirname])
disp(['Output file directory name = ',outfiledir])
disp(' ')

qcell = cell(5,1);

for s = 1:1          % Repeat for each subjects
    for c = 1:1      % Repeat for each condition
        for k = 2:6 % Repeat for each trial

            name = ['Working on : ', 's',int2str(s),
'c',int2str(c), 't',int2str(k)];
            disp(name)
            filename = ['s',int2str(s),
'c',int2str(c), 't',int2str(k), '.txt'];
            disp(filename)
            dat = dlmread([dirname,filename], '\t', 6, 0);

            t = dat(cutoff_time*record_freq+1:end,4);          % Time (s)
```

```

pitch = dat(cutoff_time*record_freq+1:end,2); % Pitch Angle
(deg)
q_v = diff(pitch)/t_step; % Angular
Velocity(deg/s)

[b,a] = butter(7,cutoff_freq*2/record_freq,'low'); % lowpass
filter coefficients
pitch_f = filtfilt(b,a,pitch); % filter the angle
q_f = filtfilt(b,a,q_v); % filter Velocity

q = [pitch_f(2:end),q_f]; % State = [pos,
vel]
qcell{k} = q;

end % k
end % c
end % s

save qcell
load qcell

ev = 5;%evolution time steps
time_step_new = -30:0.01:3;
lamda_f_new = nan(3,length(time_step_new));
for bb = 3:5

%%%%%%%%%%%%%%%%%%%%%%%%%%%%%%%%%%%%%%%%%%%%%%%%%%%%%%%%%%%%%%%%%%%%%%%%Find nearest neighbor%%%%%%%%%%%%%%%%%%%%%%%%%%%%%%%%%%%%%%%%%%%%%%%%%%%%%%%%%%%%%%%%%%%%%%%%
L2 = length(qcell{bb})-ev+1;
for ii = 1:L2
    rp = qcell{bb}(ii,:); % reference point
    q2 = [];
    for bbb = 1:6
        if bbb ~= bb
            q2 = [q2;qcell{bbb}];
        end
    end
    q21 = q2(1:end-ev+1,:);
    d = zeros(length(q21),1);

    for n = 1:length(d)
        d(n) = sqrt((q21(n,1)-rp(1))^2+(q21(n,2)-rp(2))^2);
    end
    e = min(d);
    [r,m] = find(d == e);
    % r = r;
    nn = q2(r,:);

%%%%%%%%%%%%%%%%%%%%%%%%%%%%%%%%%%%%%%%%%%%%%%%%%%%%%%%%%%%%%%%%%%%%%%%%find lamda%%%%%%%%%%%%%%%%%%%%%%%%%%%%%%%%%%%%%%%%%%%%%%%%%%%%%%%%%%%%%%%%%%%%%%%%
x1 = qcell{bb}(ii:ii+ev-1,1);
y1 = qcell{bb}(ii:ii+ev-1,2);
x2 = q2(r:r+ev-1,1);
y2 = q2(r:r+ev-1,2);
distance = zeros(1,ev);

```

```

for a = 1:ev;
    distance(a) = sqrt((x1(a)-x2(a))^2+(y1(a)-y2(a))^2);
end

t_ev = 0.01:0.01:ev*0.01;%define the evolution time
d0 = distance(1);
r_distance = log(distance/d0);
r_t_ev = t_ev-t_ev(1)*ones(1,length(t_ev));
P = polyfit(r_t_ev,r_distance,1);
lamda(ii) = P(1);
end %ii

[b1,a1] = butter(7,cutoff_freq*2/(10*record_freq),'low'); % lowpass
filter coefficients
lamda_f = filtfilt(b1,a1,lamda);
min_lamda = min(lamda_f);
mid_coordinate = find(lamda_f == min_lamda);

index = 1:L2;
time_step1 = index*t_step+(cutoff_time+1/record_freq)*ones(1,L2);
mid_point = time_step1(mid_coordinate);
time_step = time_step1-mid_point*ones(1,length(time_step1));

start_time = -30;
end_time = 3;
j = 1;
for i = 1:L2
    if time_step(1) <= start_time && time_step(end) >= end_time % long
enough
        if time_step(i) >= start_time && time_step(i) <= end_time
            lamda_f_new(bb,j) = lamda_f(i);
            j = j+1;
        end
    elseif time_step(1) > start_time && time_step(end) >= end_time %
beginning short, end enough
        empty_number = round((time_step(1)-start_time)*100);
        if time_step(i) > start_time && time_step(i) <= end_time
            lamda_f_new(bb,j+empty_number) = lamda_f(i);
            j = j+1;
        end
    elseif time_step(1) <= start_time && time_step(end) < end_time %
beginning enough, end short
        if time_step(i) >= start_time&& time_step(i) < end_time
            lamda_f_new(bb,j) = lamda_f(i);
            j = j+1;
        end
    else % both beginning and end short
        empty_number1 = round((time_step(1)-start_time)*100);
        if time_step(i) > start_time && time_step(i) < end_time
            lamda_f_new(bb,j+empty_number1) = lamda_f(i);
            j = j+1;
        end
    end
end
end
end

```

```

clear lamda

end %%bb

lamda_f_new_avg = nanmean(lamda_f_new);
st_d = nanstd(lamda_f_new);
[b1,a1] = butter(7,cutoff_freq*2/(10*record_freq),'low'); % lowpass filter
coefficients
lamda_f_new_avg_f = filtfilt(b1,a1, lamda_f_new_avg);
st_d_f = filtfilt(b1,a1, st_d);
plus = lamda_f_new_avg_f+st_d_f;
minus = lamda_f_new_avg_f-st_d_f;

figure(2)

plot(time_step_new,lamda_f_new_avg_f,'b',time_step_new,plus,'g',time_step_new
,minus,'r');
grid on
xlabel('time(s)')
ylabel('Avg lamda value')
title('NN 0.05s')

time = toc;
hours = floor(time/60/60);
mins = floor( (time-(hours*60*60))/60);
seconds = time-(hours*60*60)-(mins*60);

disp(['Time expired = ',int2str(hours),' Hours, ',int2str(mins),' Mins,
',int2str(seconds),' Seconds']);

```